THE MINERALOGICAL MAGAZINE
AND
JOURNAL OF
THE MINERALOGICAL SOCIETY

No. 217 June, 1952 Vol. XXIX

Sinhalite ($MgAlBO_4$), *a new mineral.*

(With Plate XXVII.)

By G. F. Claringbull, B.Sc., Ph.D., F.G.S., and Max H. Hey, M.A., D.Sc.

Department of Mineralogy, British Museum (Natural History).

[Read January 24, 1952.]

Introduction.

THE investigation which has led to this description of a new mineral began because of a suggestion by Dr. W. F. Foshag, when on a visit in 1951 to the Mineral Gallery of the British Museum (Natural History), that a brown cut gemstone exhibited as olivine had perhaps been incorrectly determined. More recently, Dr. Foshag has stated that the idea came from Dr. George Switzer, who as a result of an X-ray powder photograph taken in June 1950 of a similar specimen in the collection of the United States National Museum in Washington concluded that his material was not olivine and was likely to be a new species. The present work would not have been pursued had it been realized at the time that Dr. Switzer intended to continue the study when he had suitable material for analysis.

It became apparent on discussion with members of the staff of the Laboratory of the Diamond and Pearl Testing Section of the London Chamber of Commerce that both Mr. B. W. Anderson and Mr. C. J. Payne had suspected these brown supposedly iron-rich 'olivine' gemstones for many years, because their physical properties, in particular the β refractive index, did not fit the olivine graph,[1] and also because the pale colour of some of them seemed inconsistent with a high iron content.

[1] A. N. Winchell, Elements of optical mineralogy, pt. II, 1933, p. 191.

Cut stones were kindly loaned to us by the gentlemen whose names are listed in table I, and these have been extremely useful in exploring the range of properties of the new mineral. Special mention must be made of a generous gift by Mr. Robert Webster of the smaller part (76·4 mg.) of a broken stone (table I, no. 5) of the new species because it is on this material that the single crystal measurements and the chemical analysis have been made. The remainder of the stone has

TABLE I. Known specimens of sinhalite.

(Nos. 1–6 in the mineral collection of the British Museum; nos. 7–9 in the gem collection of the Geological Survey Museum.)

Serial no.	Weight in grams.	Registered number.	Previous determination.	Acquisition.
1.	3·474	B.M. 67976	Chrysoberyl renamed olivine in 1905	Purchased from W. Schmidt, 1892.
2.	4·142	B.M. 1915,315	Peridot	Presented by Lady Church, 1915.
3.	3·515	B.M. 1915,317	Peridot	Presented by Lady Church, 1915.
4.	2·038	B.M. 1934,889	Olivine	T. B. Clarke-Thornhill bequest, 1934.
5.	0·424	B.M. 1952,36	Olivine	Presented by R. Webster, 1951.
6.	0·794	B.M. 1952,37	(uncut pebble)	Presented by Dr. E. H. Rutland, 1952.
7.	0·457	5991	Chrysoberyl renamed chrysolite in 1912	Purchased from S. Henson, 1890.
8.	8·593	9821	Chrysoberyl (unchecked)	Acquired, 1912.
9.	1·619	16603	Olivine	Presented by H. Stanley Jackson, 1930.
10.	0·560	Private collection of B. W. Anderson	Olivine	—
11.	1·368		Olivine	—
12.	4·140		Olivine	Purchased from K. Parkinson, 1950.
13.	0·480		Olivine	—
14.	5·120		Olivine	Purchased from K. Parkinson, 1950.
15.	0·740	Private collection of A. E. Farn	Olivine	—
16.	0·432		Olivine	—
17.	0·440		Olivine	—
18.	0·330		Olivine	—
19.	3·700	Priv. coll. of Dr. E. H. Rutland	Olivine	—
20.	0·258	Priv. coll. of Sir James Walton	Olivine	—

now been presented by Mr. Webster to the British Museum. Further examples of the mineral were found in the collection of this Museum and also in that of the Geological Survey of Great Britain. It is pertinent to note here an entry made in 1912 by Dr. A. F. Hallimond in a register of the Geological Survey about a stone (table I, no. 7) originally called chrysoberyl and altered by him to chrysolite: 'This stone is to be further examined.'

Of the cut stones examined, two (table I, nos. 12 and 14) were brought from Ceylon in 1950 by Mr. Kenneth Parkinson and one (table I, no. 7) in the Geological Survey collection is localized as Ceylon. Confirmation of locality has been provided by Dr. E. H. Rutland, who has found a piece of rough sinhalite (table I, no. 6) in a sample of Ceylon illam imported by Chas. Matthews, Ltd. This pebble has now been presented by Dr. Rutland to the British Museum. The source of the other specimens is unknown. For this new mineral the name *sinhalite* is proposed, from Sinhala the Sanskrit name for Ceylon.

Physical properties.

The authors are grateful for permission to include in table II data determined by Mr. B. W. Anderson and Mr. C. J. Payne (nos. 5, 6, 10–20), and by Mr. E. A. Jobbins and Dr. P. A. Sabine (nos. 7–9).

Where refractive indices are recorded to four decimal places they have been measured on Abbe-Pulfrich refractometers. The comparatively small negative 2V (56° measured for the analysed specimen; calculated mean 55° from eleven determinations of refractive indices) makes relatively easy the distinction between the new mineral and olivine (2V about 90°). Pleochroism in the darker stones is α deeper brown, β green, γ lighter brown. It will be noted that the analysed specimen is one of the lightest in colour. Probably the darker stones owe their enhanced absorption to increased iron content; but since the range of refractive indices is not directly related to colour further chemical information is desirable.

Specific gravities have been determined by hydrostatic weighing in water (nos. 1–4, 7–9) or ethylene dibromide. All determinations have been corrected to water at 4° C. and rounded off to the second decimal place.

There is little difference between the hardness of sinhalite and olivine. No cleavage was observed when crushing the specimen used for chemical analysis.

TABLE II. Optical data (sodium-light) and specific gravity of sinhalite.

Serial no.	Colour.	Refractive indices.			Birefringence.	Specific gravity.
		α	β	γ	$\gamma-\alpha$	
1.	brown	1·6691	1·6984	1·7064	0·0373	3·48
2.	pale brownish-yellow	1·6667	1·6966	1·7048	0·0381	3·47
3.	pale yellowish-brown	1·6682	1·6986	1·7064	0·0382	3·47
4.	brownish-yellow	1·6693	1·7000	1·7076	0·0383	3·48
5.	yellow	—	1·6969	1·7065	—	3·48
6.	greenish-brown	1·6690	1·6993	1·7069	0·0379	3·48
7.	light brown	1·6688	1·6979	1·7051	0·0363	3·50
8.	dark greenish-brown	1·670	—	1·706	0·036	3·50
9.	pale greenish-brown	1·669	—	1·707	0·038	3·49
10.	straw-yellow	1·6670	1·6968	1·7050	0·0380	3·47
11.	light brown	1·6693	1·6981	1·7062	0·0369	3·48
12.	brown	1·6691	1·6988	1·7069	0·0378	3·48
13.	brown	1·6711	1·7002	1·7081	0·0370	—
14.	dark brown	1·6708	1·7000	1·7081	0·0373	3·50
15.	brown	1·6688	1·6985	1·7059	0·0371	—
16.	pale yellowish-green	1·6680	1·6973	1·7060	0·0380	3·48
17.	yellow	1·6708	1·6978	1·7076	0·0368	—
18.	greenish-brown	1·6765	1·7038	1·7121	0·0356	—
19.	brown	1·6680	1·6982	1·7062	0·0382	3·48
20.	pale yellow	1·6678	1·6981	1·7055	0·0377	—

X-RAY INVESTIGATION.

Powder photographs of six stones (table I, nos. 1, 5, 11, 14, 16, 18) were made in 6-cm. diam. cameras with Cu-$K\alpha$ radiation. With the exception of no. 5 the material was obtained by scraping the girdle of the cut stone with a diamond. Samples of 0·1–0·2 mg. were used in the form of roughly spherical specimens mounted on glass fibres in conjunction with cylindrical collimators. The powder diagram is remarkably constant despite the wide variation of colour.

Two X-ray powder patterns of sinhalite (table I, nos. 5 and 18) are compared in text-fig. 1 and table III with those of forsterite, olivine, and fayalite. Powder photographs of sinhalite and forsterite are reproduced in pl. XXVII.

One small brown gem olivine (B.M. 64187) thought from appearance to be sinhalite was photographed and found to give a pattern close to St. John's Island olivine; it has α 1·653, γ 1·689, sp. gr. 3·35. It must

not therefore be assumed that all brown gemstones formerly identified as olivine are sinhalite.

TABLE III. X-ray powder data for fayalite, olivine, forsterite, and sinhalite.

Fayalite		Olivine		Forsterite		Sinhalite (no. 18)		Sinhalite (no. 5)		Sinhalite (no. 5)	
$d$obs.	I.	$d$obs.	I.	$d$obs.	I.	$d$obs.	I.	$d$obs.	I.	$d$calc.	hkl.
5·26	vw	5·12	w	5·12	m	4·97	m	4·93	ms	4·94	020
4·40	vvw	—	—	4·28	vw	4·00	mw	3·97	mw	3·96	110
3·97	w	3·90	ms	3·91	s	3·77	w	3·73	vw	3·73	021
3·80	vvw	3·73	w	3·74	mw	3·45	vw	3·43	vvw	3·44	101
3·55	ms	3·49	mw	3·50	ms	3·26	s	3·24	s	3·25, 3·26	111, 120
3·05	vvw	3·00	w	3·01	m	2·84	vvw	2·82	vvw	2·84, 2·82	002, 121
2·82	s	2·77	s	2·78	s	2·64	ms	2·62	s	2·62	130
2·63	w	—	—	—	—	—	—	—	—	—	—
—	—	—	—	—	—	2·47	vvw	2·46	vw	2·46, 2·47	022, 040
2·57	ms	2·52	ms	2·52	s	2·40	m	2·38	ms	2·37, 2·38	102, 131
2·50	s	2·46	s	2·46	vs	2·32	m	2·30	ms	2·31	112
2·41	vw	—	—	2·36	vw	—	—	—	—	—	—
—	—	—	—	—	—	2·27	vvw	—	—	2·26	041
2·35	vvw	2·34	vvw	2·32	vvw	—	—	—	—	—	—
2·30	w	2·27	m	2·27	ms	2·15	vs	2·14	vvs	2·16, 2·11 2·14, 2·15	200, 210 122, 140
—	—	2·25	vw	—	—	—	—	—	—	—	—
2·193	vw	2·163	w	2·17	mw	—	—	—	—	—	—
2·070	vvw	2·032	vvw	2·04	vw	1·94	vvw	1·93	vw	1·925	132
1·982	vvw	1·952	vvw	1·96	vw	1·876 1·824	vw vvw	1·868 1·801	vw vvw	1·871, 1·863 1·808	221, 042 230
1·924	vvw	1·893	vvw	1·883	vw	—	—	—	—	—	—
—	—	—	—	—	—	1·785	vvw	1·764	vvw	1·766	023
1·840	vw	—	—	1·800	vvwb	1·716	w	1·705	w	1·707, 1·711 1·713	113, 142 151
1·776	s	1·749	s	1·751	vs	1·632	s	1·621	vs	1·625, 1·628	222, 240
1·700	vw	1·670	vw	1·673	w	1·592	vvw	1·576	vvwb	1·581	061
1·679	vw	1·640	vvw	1·642	mw	1·568	vvw			1·564	241
1·649	vw	1·620	vw	1·620	mw	1·541	w	1·534	w	1·534, 1·525	133, 232
1·626	vw	—	—	1·597	vvw					1·539	160
1·607	vvw	1·573	vvw	1·575	w	1·524	w	1·514	w	1·518	152
1·590	vvw	1·515	vvw	1·514	vvw	1·427	m	1·420	ms	1·428, 1·424	310, 203
1·535	vvw	1·498	w	1·501	ms	1·387	vvw	1·384	vw	1·385, 1·384	320, 311
1·518	m	1·480	mw	1·482	ms						
1·485	vvw	1·438	vvw	1·441	vvw	—	—	1·360	vvw	1·368, 1·364 1·351	223, 024 104
1·460	vvw										
1·430	vw	1·397	vw	1·399	mw	1·347	vw	1·340	w	1·345, 1·336	321, 114
1·420	vvw	1·350	w	1·352	m	1·324	vvw	1·320	vvw	1·321	330
1·408	vw	1·318	vw	1·318	w						
1·370	vw										
1·340	vw										

Note:—Equivalent lines of the different patterns have been arranged as far as possible in the same rows, except where these are separated by vertical rules.

Order of decreasing intensity: vvs, vs, s, ms, m, mw, w, vw, vvw; b broad. 6 cm. diameter camera, Cu–$K\alpha$ radiation (λ = 1·542 Å.). Indexing based on calculated d values from single-crystal measurements on specimen no. 5.

Despite the marked differences between the powder patterns of sinhalite and olivine there is a superficial resemblance; and subsequent

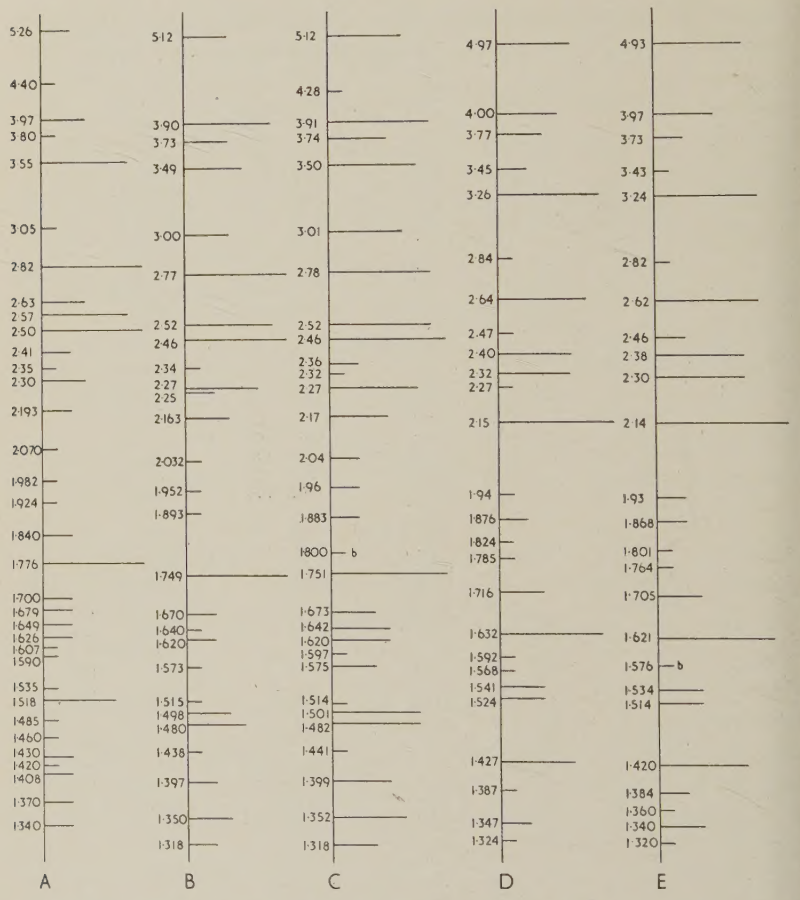

FIG. 1. Spacing intensity plots of X-ray powder photographs of: A, fayalite, Rockport, Essex Co., Massachusetts (B.M. 86609). B, olivine, St. John's Island, Red Sea, Egypt (B.M. 59305). C, forsterite, Monte Somma, Mt. Vesuvius, Italy (B.M. 80936). D, sinhalite (table I, no. 18). E, sinhalite (no. 5).

The *d* spacings are plotted as reciprocals and their approximate values in Ångström units are given against each line the length of which is an indication of intensity. *b* indicates broad and probably composite line. Data derived from table III.

indexing of these powder patterns from single-crystal data confirmed the first impression that the two minerals are related structurally. The

relationship is more clearly demonstrated by comparison of the *a*-axis Weissenberg photographs of sinhalite and forsterite (pl. XXVII, figs. 3 and 4). The structure of sinhalite is being investigated.

Single-crystal measurements for sinhalite were made from oscillation, rotation, and Weissenberg photographs of fragments of the broken stone in 6-cm. and 5·73-cm. diameter cameras. Sinhalite is orthorhombic with unit cell dimensions fairly close to olivine. The cell dimensions were refined by the method of Farquhar and Lipson[1] using back-reflection rotation photographs about the axes *a* and *c* indexed for high-order reflections by comparison with zero-layer Weissenberg photographs about the same axes. The axial ratios were first estimated from cell dimensions obtained from reflections of the type *h*00, 0*k*0, and 00*l*. The results are:

Sinhalite.		Olivine[2] ($9Mg_2SiO_4.Fe_2SiO_4$).	
a	4·328 Å.	*a*	4·755 Å.
b	9·878	*b*	10·21
c	5·675	*c*	5·985
a:*b*:*c* =	0·4381:1:0·5745	*a*:*b*:*c* =	0·4657:1:0·5862

Equi-inclination Weissenberg photographs about the *a*, *c*, and [011] axes showed the following types of diffraction spectra: *hkl* in all orders, 0*kl* only with *k* even, *h*0*l* and *hk*0 in all orders. The following space-groups are possible: D_{2h}^5 —*Pbmm*, C_{2v}^2—*Pb*2$_1$*m*, and C_{2v}^4 —*Pbm*(2).

Chemical analysis.

Sinhalite is insoluble in or only slightly attacked by acids other than hydrofluoric, differing markedly from olivine in this respect. For analysis two procedures were tried. One portion of 27 mg. was fused with sodium carbonate and the fusion distilled with methyl alcohol and sulphuric acid, the distillate being examined for boron,[3] while the residue in the flask was precipitated with 8-hydroxyquinoline, first in acetic acid solution (Al) and then in ammoniacal solution (Mg). The boron figure so obtained was suspected of being seriously low, so a second portion of 6·4 mg. was fused with caustic soda and the fusion dissolved in

[1] M. C. M. Farquhar and H. Lipson, Proc. Physical Soc., 1946, vol. 58, p. 200.

[2] W. L. Bragg, Atomic structure of minerals, 1937, p. 147; axial ratios misprinted as 0·4567:1:0·5862.

[3] E. Schulek and G. Vastagh, Zeits. Anal. Chem., 1931, vol. 84, p. 167; 1932, vol. 87, p. 195.

dilute HCl; aluminium and magnesium were precipitated together by 8-hydroxyquinoline and ammonia, and the filtrate from this precipitate was evaporated with a further addition of caustic soda and a little hydrogen peroxide, fused to complete the destruction of organic matter, and the boron titrated in the usual way; the mixed 8-hydroxyquinolates were dissolved and separated by reprecipitation in acetic acid, while iron was determined colorimetrically. This second method gave very satisfactory results. Several authors have reported difficulty in completely distilling boron as methyl borate in presence of considerable amounts of alumina.

The results of the chemical analysis are shown in table IV, together with empirical unit-cell contents calculated from the chemical analysis, specific gravity, and unit-cell dimensions. The small loss of weight on ignition has been assumed to be water, present as an impurity. The limits of probable error cited are calculated on the assumption that the cell-sides a and c are accurate to $\pm 0{\cdot}001$ and b to $\pm 0{\cdot}002$, that the specific gravity is accurate to $\pm 0{\cdot}020$ (including errors due to impurities or voids), and that the maximum probable errors of the analysis are: B_2O_3 $\pm 1{\cdot}5$, Al_2O_3 $\pm 0{\cdot}5$, Fe_2O_3 $\pm 0{\cdot}2$, MgO $\pm 0{\cdot}5$, H_2O $\pm 0{\cdot}3$. The iron was assumed to be wholly ferric; if it is all ferrous, the oxygen content will be 0·06 lower.

It will be clear that the ideal repeat formula of sinhalite is $4(MgAlBO_4)$, with an excess of Mg and Al and a deficiency of B that are probably outside the limits of error, and a small replacement of Al or Mg by Fe‴ or Fe″ (it was not possible to determine which). The calculated specific gravity for pure $MgAlBO_4$ is $3{\cdot}446 \pm 0{\cdot}001$ (the $\pm 0{\cdot}001$ arises from the uncertainties in the cell-sides), or for $MgAlBO_4$ with 0·12 atom Fe‴ replacing Al, 3·471.

TABLE IV. Chemical composition and unit-cell contents of sinhalite, and calculated percentage composition of $MgAlBO_4$. (Specimen no. 5.)

		Empirical unit-cell contents.		Calculated for $MgAlBO_4$.	
B_2O_3	24·2	B	$3{\cdot}55 \pm 0{\cdot}22$	B_2O_3	27·60
Al_2O_3	41·0	Al	$4{\cdot}11 \pm 0{\cdot}06$	Al_2O_3	40·44
Fe_2O_3	2·0	Fe	$0{\cdot}13 \pm 0{\cdot}01$	MgO	31·96
MgO	32·3	Mg	$4{\cdot}10 \pm 0{\cdot}07$		
H_2O	0·3	O	$15{\cdot}78 \pm 0{\cdot}16$		100·00
	99·8	$D_{4°}^{16°}$	3·475	$D_{4°}^{16°}$	$3{\cdot}446 \pm 0{\cdot}001$

So far as we know, no borate of Mg and Al has been obtained artifi-

Digitized by the Internet Archive
in 2023

https://archive.org/details/mineralogical-magazine_1952-06_30_217

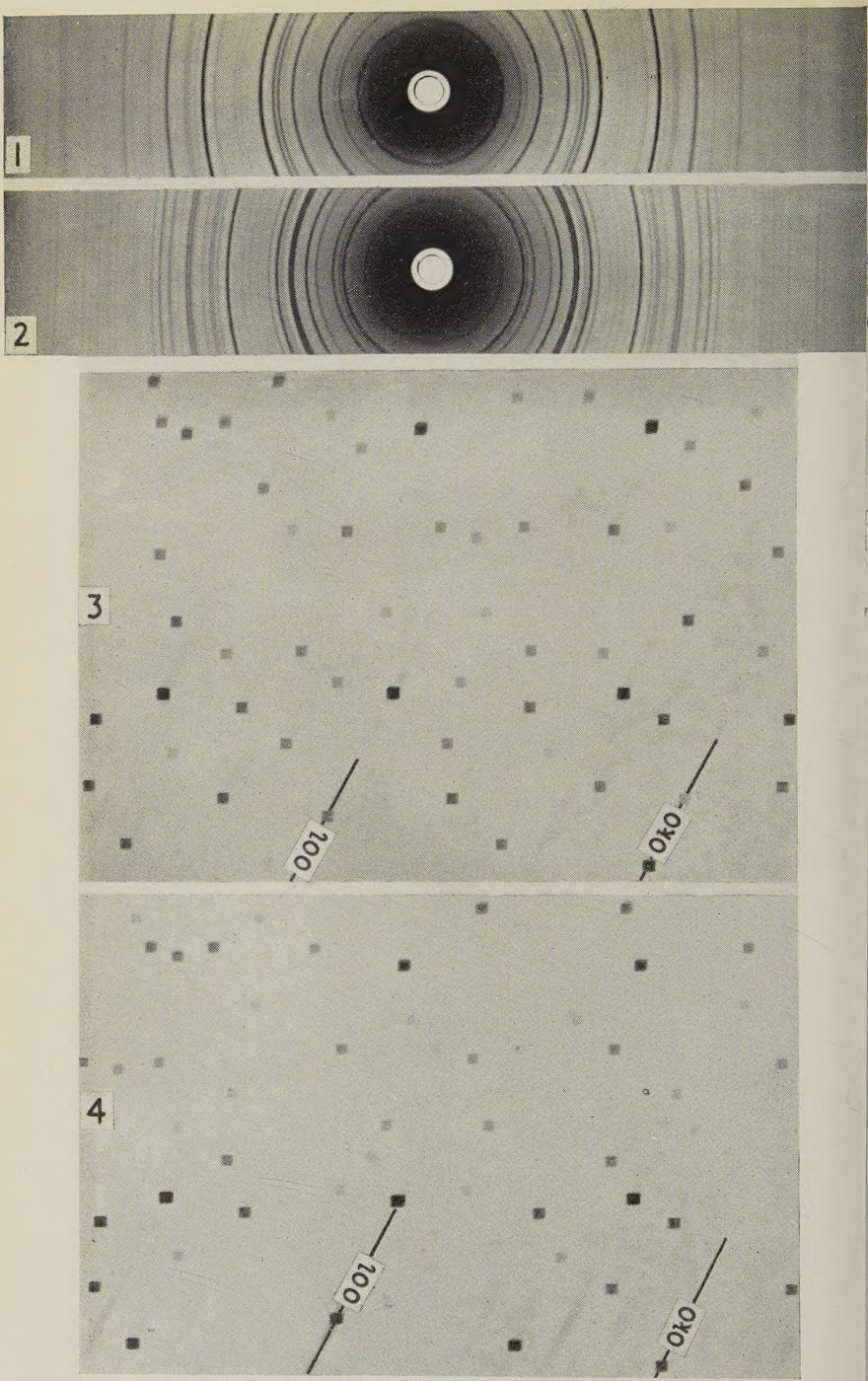

G. F. CLARINGBULL AND M. H. HEY: X-RAY PHOTOGRAPHS OF SINHALITE AND FORSTERITE

cially; a mixture of MgO, Al_2O_3, and B_2O_3 ignited at 1200° C. gradually loses all B_2O_3 by volatilization, leaving a residue of spinel.[1]

Summary.—Most of the pale yellow to deep brown gemstones previously supposed to be iron-rich olivine[2] are a new mineral, sinhalite, having the ideal formula $MgAlBO_4$. Of 22 brown and yellow stones examined 20 are sinhalite and the remaining two are close to common green olivine. Sinhalite is readily distinguishable from green olivine by its higher refractive indices and specific gravity and its much smaller optic axial angle.

Explanation of Plate XXVII.

X-ray photographs of sinhalite and forsterite. Cu-$K\alpha$ radiation (λ = 1·542 Å.).

Figs. 1 and 2. Powder photographs on 6-cm. diameter camera.

Figs. 3 and 4. Integrated Weissenberg photographs about the a-axis in 5·73-cm. diameter Nonius camera.

Figs. 1 and 3. Sinhalite (specimen no. 5, B.M. 1952, 36).

Figs. 2 and 4. Forsterite, Monte Somma, Mt. Vesuvius, Italy (B.M. 80936).

[1] J. J. Ebelmen, Ann. Chim. Phys., 1848, ser. 3, vol. 22, p. 213; 1851, ser. 3, vol. 33, p. 34.

[2] B. W. Anderson, Gem testing for jewellers, 1942, pp. 151, 183. [M.A. 8–309.]

Dalyite, a new potassium zirconium silicate, from Ascension Island, Atlantic.

By R. Van Tassel, Institut royal des Sciences Naturelles de Belgique.

With a microchemical analysis by M. H. Hey, Department of Mineralogy, British Museum (Natural History).

[Communicated by Prof. C. E. Tilley, F.R.S.; read November 1, 1951.]

EJECTED blocks of plutonic igneous facies have long been known in the trachytic and basaltic tuffs of Green Mountain and Middleton Peak on Ascension Island, and a petrographic account of them has been recorded by Professor R. A. Daly in his memoir on the geology of Ascension Island.[1]

Professor C. E. Tilley while examining thin sections of some of these rocks noticed the presence of the mineral now to be described, and following a preliminary investigation by Dr. S. O. Agrell, who also isolated the first crystal, the author was entrusted with its detailed study.

The mineral occurs as a rare accessory, about 0·2 % of the rock, in medium-grained pinkish-grey alkali-granites mainly composed of microperthite and quartz associated in varying proportions with aegirine and a strongly pleochroic green-brown alkali-amphibole. A rock specimen (B.M. 64685)[2] from Green Mountain kindly provided by the British Museum (Natural History) furnished the first mineral fragments, but most of the material was isolated from rocks preserved at Cambridge[3] (Harker slide collection nos. 57069, 57219).

The mineral is now shown to be a potassium zirconium silicate for which the name *dalyite* is proposed in honour of Reginald Aldworth Daly (1871–), Emeritus Professor of Geology, Harvard University, who

[1] R. A. Daly, The geology of Ascension Island. Proc. Amer. Acad. Arts & Sci., 1925, vol. 60, no. 1, pp. 1–80 (see pp. 63–68). [M.A. 3–385.]

[2] This rock specimen was collected during the cruise of H.M.S. Challenger, 1873–6, and is described by A. F. Renard in the Challenger Report as amphibolic granite. Report on the petrology of Oceanic Islands, 1889, pp. 63–64.

[3] For these and numerous other specimens of ejected blocks on Green Mountain and Middleton Peak the Department of Mineralogy and Petrology at Cambridge is greatly indebted to the Manager of Cable and Wireless Ltd., Ascension Island, who on my inquiry, through the kind offices of the Directorate of Colonial Geological Surveys, arranged for the collection of this material. Grateful acknowledgement is due to Messrs. M. A. Miles, H. W. Benjamin, and G. A. O'Dean, members of the Company's staff, who were responsible for the field work.—C. E. Tilley.

has contributed so much to our knowledge of the geological structure and petrology of Ascension Island.

Rough crushing of the rather friable rock, concentration with suitable heavy liquids, and careful hand-picking under the microscope provided about 100 mg. of pure material.

Dalyite forms colourless, completely transparent, triclinic crystals ranging 0·1 0·5 mm. in size, with short prismatic habit and vitreous lustre. Cleavage directions are observed and twinning is not uncommon. The hardness is about $7\frac{1}{2}$, the mineral just scratching quartz. The principal properties of dalyite are described below under separate headings.

Unit cell.

The unit cell of dalyite was determined from X-ray photographs using copper radiation with a nickel filter. A small crystal $0{\cdot}25 \times 0{\cdot}3 \times 0{\cdot}35$ mm. in size, of which fig. 1A is a true representation, was mounted in a Weissenberg camera of 3 cm. radius and having 2° rotation for 1 mm. traverse. The well-developed prism was set parallel to the rotation axis of the instrument. The equatorial layer was recorded with a normal beam photograph and the first and third layer-lines with equi-inclination photographs. As the reciprocal net constructed from the zero layer-line photograph is non-orthogonal and as adjacent layer-lines do not superpose on it, triclinic symmetry is at once revealed. The cell constants have been chosen in order to give the smallest cell as nearly orthogonal as possible and to satisfy the conventional rule, $c<a<b$, α and β obtuse.[1] From the third layer-line, the oscillation photograph gave c 7·00 Å. The reciprocal cell constants, obtained from Weissenberg photographs, are: for the equatorial layer-line a^* 0·236, b^* 0·219, and γ^* $71\frac{1}{2}°$; for the first layer-line, with beam inclination μ 6° 20′, a^* 0·235, b^* 0·218, and γ^* $72\frac{1}{2}°$; and for the third, with inclination μ 19° 20′, a^* 0·233, b^* 0·218, and γ^* 72°. From these data were deduced the average values a^* 0·235, b^* 0·218, and γ^* 72°. Graphically the following constants were also obtained: c^* 0·259, α^* 68°, and β^* 62°.

The Bravais cell constants, calculated from the preceding data, are a 7·51, b 7·73, c 7·00 Å., α 106°, β $113\frac{1}{2}°$, and γ $99\frac{1}{2}°$. The accuracy for the linear values is $\pm$ 1% and for the angles $\pm 1°$. The calculated volume of this unit cell is 341 Å^3. As the specific gravity determined on the same crystal, by suspension in liquids of known density, is $2{\cdot}84 \pm 0{\cdot}02$, the calculated molecular weight, or a multiple of it, is about 582.

[1] J. D. H. Donnay, Rules for the conventional orientation of crystals. Amer. Min., 1943, vol. 28, pp. 313–328. [M.A. 9–140.]

Morphology.

Twenty-three crystals, all of incomplete crystallographic outline, were measured on the two-circle goniometer. Confirming the triclinic character shown by X-rays, a centre is the only element of symmetry observed. Hence the crystal class is $\bar{1}$ and the space-group $P\bar{1}$. The unit cell

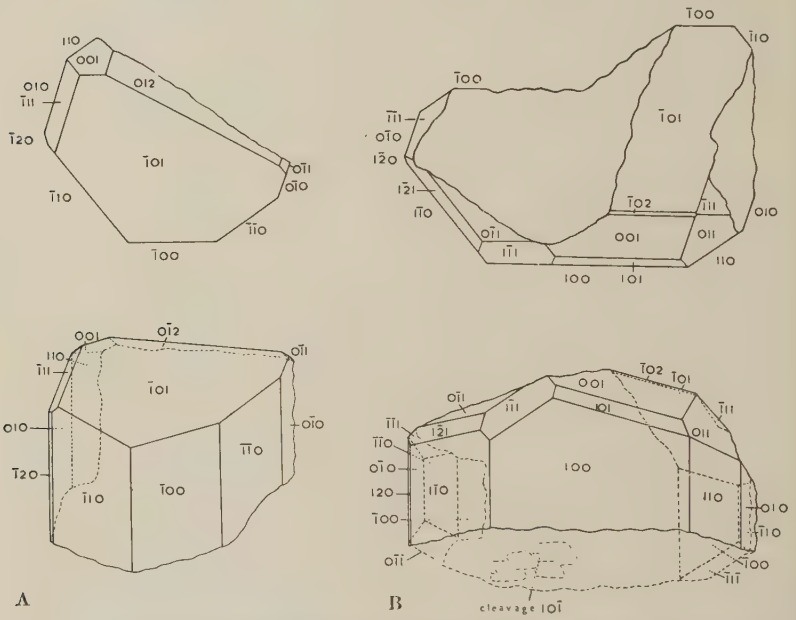

FIG. 1. Top and side views of dalyite crystals in true representation. A, 0·25 × 0·3 × 0·35 mm.; B, 0·25 × 0·45 × 0·5 mm.

deduced from X-ray data served for the assignment of the face indices. Sixteen crystal-forms were identified; they are tabulated below together with the frequency of their observed occurrence:

{100}	{010}	{001}	{$\bar{1}$01}	{110}	{1$\bar{1}$0}	{1$\bar{2}$0}	{$\bar{1}$11}
19	11	6	21	11	13	6	10
{011}	{101}	{$\bar{1}\bar{1}$1}	{1$\bar{2}$1}	{1$\bar{1}$1}	{0$\bar{1}$1}	{$\bar{1}$02}	{0$\bar{1}$2}
2	2	5	4	6	4	2	1

The frequency figures have only a limited value as all the measured crystals were broken fragments. Whenever more or less complete, the crystals show short-prismatic habit. The form {$\bar{1}$01} is most frequent and produces also large faces with excellent reflection. This behaviour suggests another choice for the *z*-axis and the assignment of {001}

indices to the form, but in view of the X-ray data and the conventional rules, the indices tabulated above are assigned in the present study. The forms {1$\bar{1}$0} and {100} are also important; somewhat less so are {010} and {110}, while {1$\bar{2}$0} is narrow. {001} is irregular in behaviour. The forms {$\bar{1}$11}, {0$\bar{1}$1}, {1$\bar{1}$1}, {1$\bar{2}$1}, {011}, and {1$\bar{1}$1} usually produce small good faces; {101} and {$\bar{1}$02} are narrow. The form {0$\bar{1}$2} is rather doubtful as it has only once been observed with bad reflection. The good cleavages are {$\bar{1}$01} and {010}, and less distinct {100}.

Two-circle goniometer angles, measured on the two most complete crystals, shown in fig. 1, are given in table I.

TABLE I. Measured two-circle angles of dalyite.

	Crystal A.			Crystal B		
Face.	ρ.	ϕ.	Reflection.	ρ.	ϕ.	Reflection.
(101)	—	—	—	58° 14′	27° 51′	bad
(100)	—	—	—	90 15	17 38	perfect
(001)	31° 00′	46° 01′	bad	30 59	46 25	good
(110)	89 40	51 59	good	89 54	51 55	good
(010)	89 33	90 00	good	89 54	90 00	good
($\bar{1}$02)	—	—	—	17 —	106 —	very bad
($\bar{1}$11)	51 22	118 48	good	50 54	118 45	good
($\bar{1}$20)	90 03	121 11	bad	—	—	—
($\bar{1}$10)	89 43	146 46	good	90 04	147 00	bad
($\bar{1}$01)	31 26	169 12	perfect	31 14	169 35	good
($\bar{1}$00)	89 57	197 20	good	90 04	197 36	good
($\bar{1}\bar{1}$1)	—	—	—	−56 02	170 24	good
($\bar{1}\bar{1}$0)	90 03	232 02	good	90 07	232 25	good
($\bar{1}\bar{1}$1)	—	—	—	46 34	235 45	good
(12$\bar{1}$)	—	—	—	−55 37	253 26	good
(0$\bar{1}$0)	90 03	269 46	good	90 19	270 17	good
(0$\bar{1}$1)	34 49	306 41	bad	—	—	—
(1$\bar{2}$0)	—	—	—	90 29	301 45	bad
(1$\bar{1}$0)	—	—	—	90 29	327 30	good
(12$\bar{1}$)	—	—	—	62 14	319 39	good
(1$\bar{1}$1)	—	—	—	55 36	350 47	good
(10$\bar{1}$)	—	—	—	−31 —	355 —	bad (cleavage)
(0$\bar{1}$2)	21 57	319 01	very bad	—	—	—

The better readings, selected among the available data on all the measured crystals, were used for the calculation of the axial angles and ratios:

	Limits.	Number.	Average.
($\bar{1}$00) ($\bar{1}$01)	62° 32′–62° 45′	8	62° 38′
($\bar{1}$10) ($\bar{1}$01)	60 53–61 06	7	61 01
($\bar{1}$10) ($\bar{1}$00)	50 30–50 46	5	50 37
(001) ($\bar{1}$01)	53 57–54 16	4	54 05
(100) (010)	72 30–72 39	6	72 33

$a:b:c = 0{\cdot}958:1:0{\cdot}899$, α 106° 19′, β 112° 25′, γ 99° 08′.

These goniometric data are in satisfactory agreement with the cell constants obtained from X-rays:

$$a:b:c = 0{\cdot}970:1:0{\cdot}906,\ \alpha\ 106°,\ \beta\ 113\tfrac{1}{2}°,\ \gamma\ 99\tfrac{1}{2}°.$$

Table II summarizes a selection of interfacial angles (mean values), measured on the crystals and calculated from the established parameters.

TABLE II. Measured and calculated interfacial angles of dalyite.

	Meas.	Calc.		Meas.	Calc.
(001) (100)	63° 27′	63° 17′	(001) ($\bar{1}$11)	48° 33′	48° 50′
(001) (010)	68 09	68 01	($\bar{1}$01) ($\bar{1}\bar{1}$1)	42 21	42 17
(100) (110)	37 57	37 57	(001) ($\bar{1}\bar{1}$1)	77 15	77 15
(110) (010)	34 36	34 36	(001) (0$\bar{1}$1)	48 43	48 45
($\bar{1}$10) ($\bar{1}$20)	25 07	25 10	($\bar{1}$01) (1$\bar{2}$1)	90 00	90 03
($\bar{1}$10) (010)	56 53	56 50	(001) (1$\bar{2}$1)	64 50	64 37
($\bar{1}$01) ($\bar{1}\bar{1}$0)	76 18	76 19	($\bar{1}$01) (1$\bar{1}$1)	86 49	86 51
(001) (110)	59 04	59 10	(001) (1$\bar{1}$1)	43 26	43 24
($\bar{1}$01) ($\bar{1}$20)	69 05	69 13	(001) (101)	29 58	30 01
(001) ($\bar{1}$20)	82 42	82 22	($\bar{1}$01) (101)	84 03	84 06
($\bar{1}$01) ($\bar{1}$11)	37 31	37 33	(001) ($\bar{1}$02)	26 38	27 08

Twinning is not rare, as among the 23 crystals isolated for goniometric measurements, four were twinned. They form normal twins with (100) as composition plane. Some of the measured angles (single readings) are compared with the calculated values:

	Meas.	Calc.		Meas.	Calc.
($\bar{1}$01) ($\underline{\bar{1}01}$)	54° 40′	54° 44′	($\bar{1}$11) ($\underline{\bar{1}11}$)	17° 42′	17° 34′
(001) ($\underline{001}$)	53 04	53 26	($\bar{1}$10) ($\underline{\bar{1}10}$)	78 54	78 46
(010) ($\underline{010}$)	35 03	34 54	(110) ($\underline{110}$)	110 24	110 48

Optical properties.

The refractive indices determined by the immersion method are α 1·575, β 1·590, γ 1·601, all $\pm$0·002. The optic axial angle measured on the universal stage is negative with 2V 72°$\pm$2°. Dispersion is very weak with presumably $v<r$. Using crystals with identified faces the optical orientation was determined on the universal stage: α, acute bisectrix, is nearly parallel to the c-axis ($\alpha:c = 7°$), and the axial plane forms an angle of 18° with (100), which is also the twin plane. Fig. 2 illustrates the crystallographic and optical orientation.

Inclusions are occasionally observed in the crystals of dalyite: (1) isotropic, highly refractive, orange, transparent octahedra of 60–100μ; (2) swarms of very thin needles of rutile (?), and small cavities with crystalline outline of 8–40μ are present, often filled with a bubble. The octahedral mineral, isolated by Dr. S. O. Agrell, has a cell size of

10·4 Å. as determined from X-ray oscillation photographs and is to be regarded as a member of the pyrochlore group.

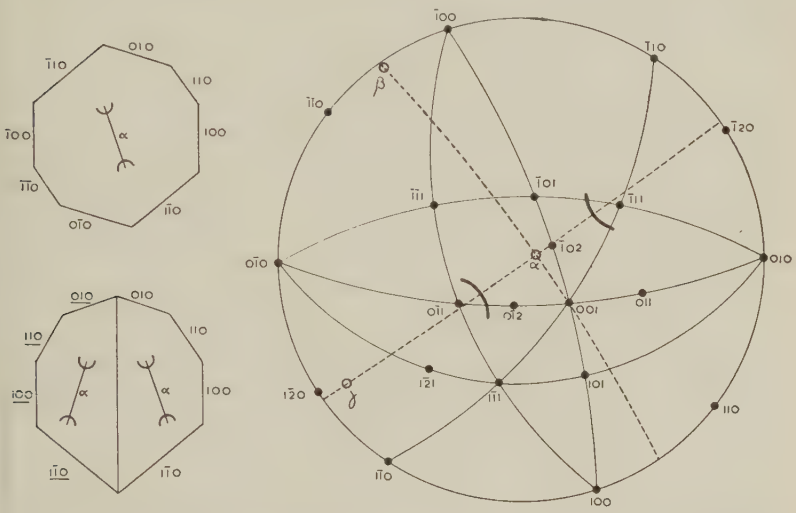

FIG. 2. Stereographic projection of crystal forms and optical orientation, and ideal sections perpendicular to the prism zone in single and twin crystals. $\alpha : c = 7°$.

Chemical composition.

The small amount of available material required special care and the use of micro-methods. Spectrographic investigation, based on arc emission and on visual evaluation of step-sector spectrograms, permitted a semi-quantitative determination. Mixtures of known and similar composition were prepared for comparison and only mineral fragments individually tested and optically free from inclusions, were selected for arcing. Potassium, zirconium, and silicon are the main constituents. Sodium was estimated at about 1% Na_2O. Be, Mn, Sr, Li, Cs, Rb, and F were not detected (limit of sensitivity about 0·001%, except for Cs and F 0·05 %). Other elements were identified, but occur only in negligible amounts.

The evaluation of absolute line intensities permitted the determination of the main constituents, within the stated limits of error, as follows: K_2O 16±3 %, ZrO_2 20±5 %, SiO_2 55±6 %. These constitute almost exclusively the whole mass and molecular ratios based on these figures are K_2O 1·05±0·2, ZrO_2 1±0·25, SiO_2 5·6±0·6. In addition, the neighbouring lines Si 2987–Zr 2985 provide a suitable pair for relative evalua-

tion according to the internal method. In this way the ratio $ZrO_2:SiO_2$ is found to be $1:5{\cdot}5\pm0{\cdot}5$. A compound with the formula $K_2O.ZrO_2.5SiO_2$ has in its simplest expression a molecular weight of 517·7 against 577·8 for $K_2O.ZrO_2.6SiO_2$. As the figure of 582 was determined from X-ray data, the latter formula appears quite probable, hence the unit cell contains one molecule.

The conclusions drawn from the spectrographic data are satisfactorily supported by a microchemical analysis subsequently completed by Dr. M. H. Hey on 22 mg. of the mineral. The interpretation of the analytical results given in table III leads to the formula $K_2ZrSi_6O_{15}$, where sodium replaces a part of the potassium. Zirconium was weighed as ZrO_2 and any hafnium will not alter sensibly the molecular ratio $SiO_2:(Zr,Hf)O_2:K_2O$, as the zirconium content, spectrographically determined on characteristic lines, cannot be less than 15 %. Dr. Hey has preserved the crude ZrO_2 and hopes eventually to have the Hf:Zr ratio determined.

Table III. Microchemical analysis of dalyite.

		Mol. ratios.	Oxygens.	Metals.	Metals on a basis of 15O.
SiO_2	61·85	1030	2060	1030	5·95	
ZrO_2	21·70	176	352	176	1·01	
K_2O	14·60	155	155	310	1·79	2·11
Na_2O	1·75	28	28	56	0·32	
Fe_2O_3	0·37	—	—	—	—	
H_2O	0·64	—	—	—	—	
	100·91					

Dalyite is unaffected by warm concentrated nitric acid but is slowly attacked by cold, and readily dissolved by hot hydrofluoric acid. Only when the full heat of a mekker burner is applied does dalyite show a change. Under this treatment very tiny, highly refringent prisms with straight extinction and positive elongation (? zircon) appear along with glass. Dalyite is chemically most nearly related to wadeite,[1] but it is much richer in silica and simpler in composition. Moreover, the crystallographic properties are entirely different.

Powder pattern of dalyite.

For identification purposes an X-ray powder photograph has been taken using copper radiation with nickel filter on a camera of 19 cm. diameter. A print is reproduced in fig. 3. As the pattern is very com-

[1] R. T. Prider. Some minerals from the leucite-rich rocks of the West Kimberley area, Western Australia. Min. Mag., 1939, vol. 25, pp. 373–387.

plex the weaker reflections have been omitted in table IV, which summarizes the measured spacings and the visual intensities.

TABLE IV. X-ray powder data for dalyite.

d.	Int.	*d*.	Int.	*d*.	Int.
6·54	m	2·85	m	1·840	w
5·90	s	2·66	w	1·791	w
4·31	s	2·62	vs	1·675	w
4·20	vs	2·42	m	1·640	w
3·65	w	2·25	w	1·469	w
3·58	vs	2·21	w	1·467	w
3·36	m	2·15	w	1·312	w
3·26	w	2·09	w	1·282	w
3·08	vs	2·07	w	1·211	w

(vs, very strong; s, strong; m, medium; w, weak)

FIG. 3. X-ray powder photograph of dalyite. ($\times\frac{2}{3}$.)

Acknowledgements.—This study was carried out in the Department of Mineralogy and Petrology, Cambridge, while holding a British Council Scholarship. The author wishes to thank Professor C. E. Tilley for bringing the problem to his notice and for reading the manuscript. He also desires to thank Drs. S. O. Agrell, N. F. M. Henry, S. R. Nockolds, and W. A. Wooster for advice, and Mr. R. S. Allen and Mr. K. O. Rickson for technical assistance.

Summary.—Dalyite ($K_2ZrSi_6O_{15}$), a new mineral, occurs in ejected blocks of alkali-granite from Ascension Island. It forms small colourless triclinic crystals with $a:b:c$ — 0·958:1:0·899, α 106° 19′, β 112° 30′, γ 99° 08′. Absolute parameters: a 7·51, b 7·73, c 7·00 Å., Class $\bar{1}$, space-group $P\bar{1}$. Sixteen forms: {100}, {010}, {001}, {$\bar{1}$01}, {110}, {1$\bar{1}$0}, {1$\bar{2}$0}, {$\bar{1}$11}, {011}, {101}, {$\bar{1}\bar{1}$1}, {1$\bar{2}$1}, {1$\bar{1}$1}, {0$\bar{1}$1}, {$\bar{1}$02}, {0$\bar{1}$2}. Cleavages ($\bar{1}$01) and (010). Normal twinning with (100) as composition plane. Optical constants: α 1·575, β 1·590, γ 1·601, $2V_\alpha$ 72°, $\alpha:c$ — 7°, axial plane to (100) = 18°. Unit cell [$K_2ZrSi_6O_{15}$]. Density 2·84. Hardness 7½.

The growth and properties of large crystals of synthetic quartz.

By C. S. Brown, R. C. Kell, and L. A. Thomas

Research Laboratories of The General Electric Company, Limited, Wembley.

Nora Wooster and W. A. Wooster

Brooklyn Crystallographic Laboratory, Cambridge.

[Read January 24, 1952.]

Introduction.

In the last twenty years quartz has become of considerable importance to the telecommunications industry, one of its most important uses being the control of the frequency of oscillation of high-frequency transmitters. In this country alone the peak war-time demand for oscillator crystals was well over a million a year.

Although quartz is very abundant in the earth's crust it is usually found in the polycrystalline state or as small crystals. Large crystals, reasonably free from twinning and flaws, are relatively rare and most of the supply for piezoelectric purposes comes from Brazil.

Attempts have been made to grow synthetic quartz for over a century, but, except for the work of Spezia in 1900, they resulted only in the production of minute crystals. The scarcity of high-grade Brazilian quartz during the war presented a new aspect to this problem and in the early 1940's work began both in this country and in Germany, and more recently it has also been followed in the U.S.A.

History of the preparation of quartz crystals.

Schafhäutl (1845) produced microscopic hexagonal crystals of quartz by heating freshly precipitated silica in Papin's digester for eight days. Many variants of this experiment were subsequently carried out by geologists and mineralogists. Mineralizers added, in an effort to improve quality and size, included hydrochloric acid (de Sénarmont, 1849, 1851), carbonic acid (de Sénarmont, 1851), and hydrofluoboric acid (von Chroustschoff, 1887). Most of these experiments were conducted at

temperatures between 200° and 300° C., and many lasted several months. Other hydrothermal methods that were tried included Daubrée's (1859) interesting experiment of heating glass tubes in water in an autoclave. He obtained a kaolin-like mass in which doubly-terminated, perfect quartz crystals were embedded. This result was confirmed by Bruhns (1889) who added ammonium fluoride as a mineralizer. All these experiments were successful in producing quartz crystals, often of good quality, but the crystals were invariably small and usually microscopic.

Spezia (1900–1909), however, carried out a series of experiments which showed that large crystals could be grown in the course of a few months provided an adequate source of raw material was available. His method was based on the fact that quartz is more soluble in a solution of sodium metasilicate at temperatures above 300° C. than below it. His apparatus consisted of an autoclave which was heated by gas at the top and cooled by water at the bottom. The extremes of temperature that he obtained on the outside of the autoclave in a typical experiment were between 326° and 337° C. at the top, and 165° and 178° C. at the bottom. A silver wire basket containing quartz chips was placed in the hot part of the autoclave and a truncated quartz crystal was suspended some distance below. As a result of the quartz chips dissolving the density of the solution around the basket increased and the heavy liquid flowed down past the seed crystal. This being at a lower temperature, the liquid became supersaturated, and the seed grew. After one typical experiment had been in progress some hundred days, Spezia quenched the bomb and opened it. He found the two truncated crystals he had inserted had grown complete rhombohedral terminations, and the crystals had increased in weight by 97 and 79 %. One of Spezia's crystals is shown in fig. 1. He found that quartz crystals grown in a simple sodium metasilicate solution were cloudy, but that if he added 'a handful' of sodium chloride, the quality was excellent.

Day and Shepherd (1906) published some experiments which showed that quartz could be obtained by heating magnesium ammonium chloride with sodium metasilicate and water in a steel bomb to 400° or 450° C. for three days. Only small crystals were obtained. Fenner (1912, 1914) heated silica glass or amorphous precipitated silica with water and sodium carbonate in a steel bomb at a temperature between 400° and 500° C. for two or three days, and obtained perfect doubly-terminated crystals 2 or 3 mm. long.

Two of the authors, Wooster and Wooster (1946), set up an apparatus

similar in all respects to that used by Spezia and carried out a number of tests on the growth and solution of silica in the form of quartz, silica glass, and soda glass. The result obtained by Spezia that quartz could be grown on a seed crystal in the cooler part of an autoclave when a source of quartz was present in the hotter part, was confirmed. The rate of growth obtained was so slow that the process did not appear promising. At the same time it was found that silica glass was considerably more soluble in sodium metasilicate than broken crystalline quartz. Minute crystals of quartz are readily obtainable from the devitrification of silica glass under these conditions, but attempts to grow large crystals by allowing only one nucleus to develop were unsuccessful. This work, however, led to a new process for growing large crystals of quartz, which depended on the greater solubility of silica glass compared with that of quartz under hydrothermal conditions. In an autoclave containing both silica glass as source material and quartz seeds, the solution could be saturated with respect to the vitreous phase and supersaturated with respect to the crystalline seed, on which growth of quartz would consequently ensue. The process could thus be carried out under isothermal conditions, the temperature gradient used by Spezia being unnecessary. Growths of up to 0·5 mm. on each side of a seed plate cut parallel to a major rhombohedral face ($10\bar{1}1$) were obtained in a run of about a day. Due to the very high supersaturation obtained in this isothermal process, spurious seeding occurred on the wall of the bomb and a large part of the source devitrified in situ. Increasing the amount of source only increased the amount that devitrified and did not increase the amount available for deposition on the seed. Thus the run could not be increased beyond a day and to grow a large crystal the autoclave had to be frequently recharged and the growth built up in layers. It has been found that during the initial stages of each cycle of growth there is a thin disordered layer which is clearly visible under the microscope.

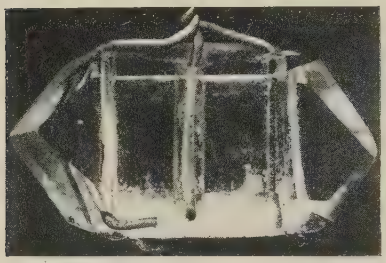

Fig. 1. Quartz crystal showing pyramidal terminations, grown by G. Spezia in 1906, on a truncated prism of natural quartz as seed (with supporting wire). ×4. (Kindly loaned by the University Museum, Oxford.)

Numerous attempts have been made to overcome the discontinuous

nature of the isothermal process but these have met with little success. In one of these attempts, a method of circulating a silica-saturated solution at high pressure from one chamber containing the source to another containing the seed crystals was tried.

The high supersaturation encountered in the isothermal process gives rise to very variable results and it has been found to be extremely

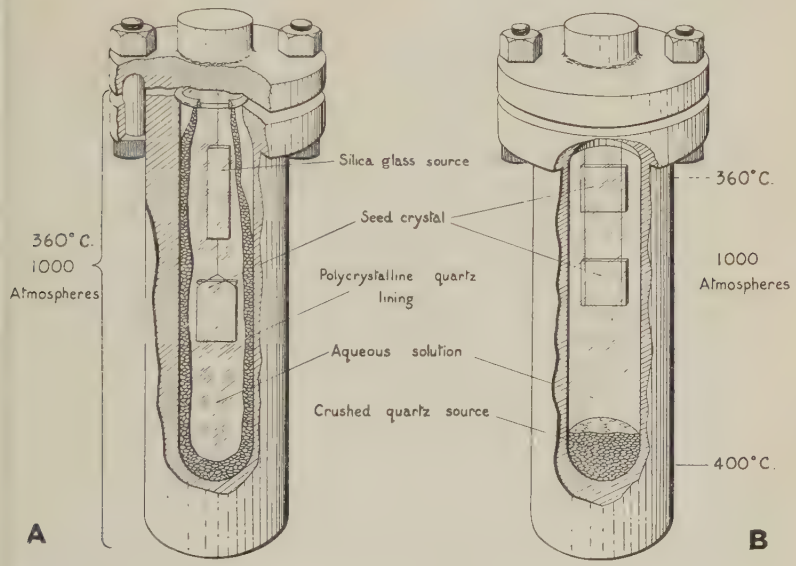

FIG. 2. Autoclaves showing the difference of arrangement in the isothermal (A) and temperature-gradient (B) methods.

difficult to produce a thick layer of quartz which shows no imperfections (Thomas, Wooster, and Wooster, 1949). This variability and the discontinuous nature of the process have led to a method based on the temperature-gradient process of Spezia being preferred. This possesses the advantages of a readily controllable supersaturation and gives a continuous growth of high quality. A diagram comparing the arrangements in the autoclaves in the isothermal and temperature-gradient methods is shown in fig. 2.

Independent of the work carried out in this country, Nacken (1945) devised a process similar to the isothermal method which we had used. Nacken's work ceased in 1944 but was taken up by workers in the U.S.A. After their early attempts at overcoming the difficulties of the isothermal technique had failed, Hale (1948, 1949) and Walker and

Beuhler (1950) started using a form of temperature-gradient-technique which, although similar to that described in the following section, possesses certain significant differences. These have been briefly discussed by Brown et al. (1951).

Growth of large crystals.

The work reported here has been carried out using autoclaves 10 inches long with an internal diameter of 2 inches and walls a little over $\frac{3}{4}$-inch thick. Mild steel, durahete steel, and S.80 stainless steel have all been used successfully, although the superior strength of the two latter materials has proved advantageous. The autoclaves are sealed using a mild steel lens ring. When the lid is bolted to the body of the autoclave with eight bolts of high tensile steel, a line contact occurs between the spherical surfaces of the lens ring and the conical surfaces turned on the lid and body. In this manner the autoclaves have been sealed to withstand pressures approaching 2000 atmospheres.

The furnaces used are simple but effective and consist of a hot plate on which the autoclave stands, completely surrounded by broken refractory material for thermal insulation, as shown in fig. 3.

The temperatures at various points of the autoclave are measured by strapping on thermocouples. The temperature at the base is controlled to within $\pm 1°$ C. using a mechanical temperature-regulator, whilst the top is allowed to attain an equilibrium temperature some 40° C. lower than that at the base. Detailed measurements of the temperature distribution have shown that a large part of this temperature drop occurs in the metal forming the base of the autoclave and that the temperature gradient in the liquid is certainly less than $\frac{1}{2}°$ C./inch. This small gradient in the liquid enables crystals of comparable size to be grown throughout the length of the autoclave.

The pressure developed under working conditions is controlled primarily by the temperature and the initial degree of filling of the liquid in the autoclave. The liquid used is a 10 % sodium carbonate solution in water.

The source material which maintains the supersaturation of the liquid with respect to silica in the vicinity of the seed crystals is in the form of melting-quality quartz which has been crushed in a mechanical ore crusher. The size of the particles of the source material is an important factor affecting the rate of growth and hence the quality of the synthetic crystals. The quartz used as source is of comparatively low cost since it can be of small size and the presence of flaws and twinning is immaterial.

The seed crystals are cut in the form of rectangular plates, approximately 2 mm. thick, and are suspended from the lid of the autoclave by fine platinum wires looped round the seeds near the edges. The seeds hang with the major surfaces vertical to avoid the deposition of rubble on the growing faces. The orientation of the seed plate with respect to

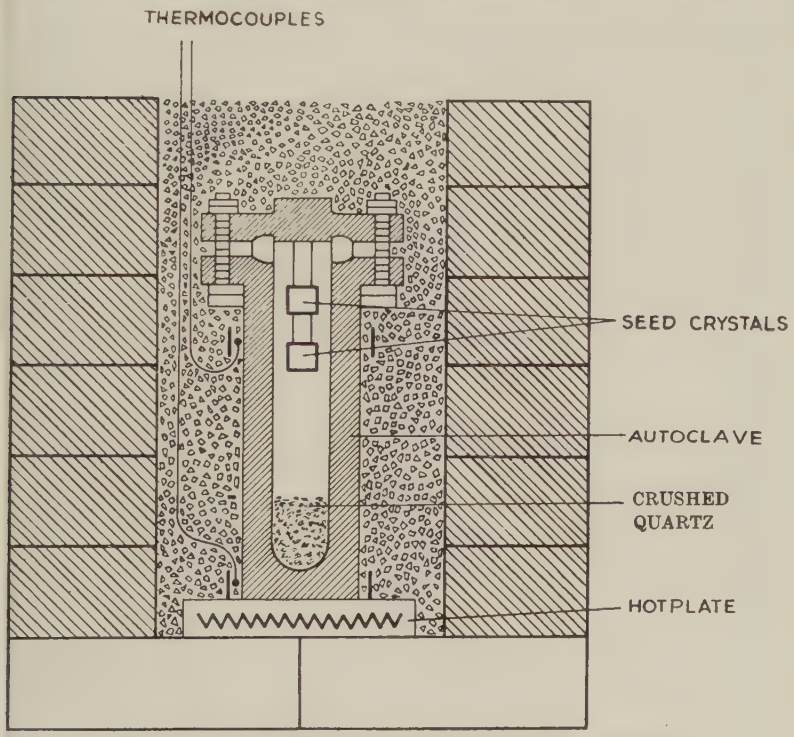

FIG. 3. Furnace arrangement in the temperature-gradient method.

the crystallographic axes is of considerable importance, the form of the final crystal and the rate at which it grows being dependent upon it. The majority of the experiments have been carried out using plates cut parallel to the basal plane (0001), although plates cut parallel to both positive and negative rhombohedral faces have been used.

Early experiments, using the temperature-gradient process, soon showed that the growth on the basal plane, although not a natural form face, can be of good quality as long as the growth rate is controlled to be less than a critical value. This contrasts with the results published by Hale (1948) and Walker and Beuhler (1950) who have reported that

the growth is usually misoriented and filled with inclusions until the crystal is completely 'capped', that is, until the pyramid has fully developed and the basal plane has disappeared. This poor quality capping is similar to that which occurs in the growth of water-soluble crystals, such as ethylene diamine tartrate and ammonium dihydrogen phosphate. Much of the work since these early experiments has been directed towards an understanding of the factors affecting the quality and rate of growth of crystals grown in this manner. It has been found that the walls of the autoclave must be scrupulously clean before the start of an experiment or else small crystals of quartz will develop on the walls and result in a considerably reduced rate of growth. (In the earlier isothermal method the presence of a thick lining of polycrystalline quartz was essential for clear growth.) If the supersaturation is too high, spontaneous nucleation will occur on the wall of the autoclave however clean it is and the quartz deposited on the seed crystals will tend to become less perfect. The reproducibility of the process is such that the time and conditions of a growth run to produce a given size of crystal can be predicted reasonably accurately as long as the growth rate is kept below the critical value. The crystals grown under optimum conditions are free from all flaws and twinning.

The critical rate of growth, above which the quality of the quartz deposited is no longer perfect, is itself a function of the process variables and has been considerably increased since the beginning of this work. In a full-length run it is now possible to deposit quartz at an average rate of 0·6 mm./day in the direction of the optic axis on each side of the seed without any visible defects occurring. The characteristics of the process are such that this involves a maximum rate of growth in excess of 1·0 mm./day. In this manner crystals weighing up to 150 grams and with growths up to 16 mm. on each side of the seed have been grown in about four weeks. Fig. 4 shows such a crystal, together with a similar growth on a seed crystal of somewhat smaller area. This growth is the largest that can be obtained in the 2-inch bore autoclaves without the crystal coming into contact with the wall. However, it is remarkable that the growth is still of good quality even when the fully-grown crystal nearly fills the bore of the autoclave. Crystals more closely resembling the development of natural crystals can be obtained by growing on to seeds of smaller area. Two crystals grown on 2 cm. square seeds are shown in fig. 5 and these crystals have been very nearly completely capped.

The quality of a typical synthetic crystal is shown in fig. 6 by a

photograph of a crystal immersed in benzene, which was chosen because its refractive index differs sufficiently from that of quartz for some relief to be visible. There is no sign of any flaws or inclusions and the seed/growth interface cannot be discerned. A similar photograph (not reproduced here) was taken in methyl salycilate. This liquid very closely

Fig. 4. Synthetic quartz crystals (150 and 70 grams). The mottling is due to the large cobbled surfaces approximating to basal planes. ×0·6.

Fig. 5. Synthetic quartz crystals almost completely capped by rhombohedral faces. ×1·2.

matches the mean refractive index of quartz and all that could be seen were the supporting wires and the reference number written on the crystal surface.

Above the critical rate of growth, the quality of the quartz deposited becomes steadily worse. At very rapid rates of growth the quartz is deposited as a large number of small pyramids having the appearance of a drusy mineral. Liquid may be included in gaps in the deposit so as to give the crystal an opaque appearance. However, far less obvious flaws can occur and these may still be sufficient to make the crystal unsuitable for the manufacture of oscillator plates. Some crystals which

appear to be visually perfect show marked Tyndall scattering in a high-intensity light beam. From the distribution of the intensity of the scattered light it has been inferred that the flaws causing the scattering are less than $0{\cdot}1\lambda$ and may even be of the order of molecular dimensions. These minute flaws have been found sufficient to spoil the performance of high-frequency oscillator plates. Slight reduction in the rate of growth has overcome this defect.

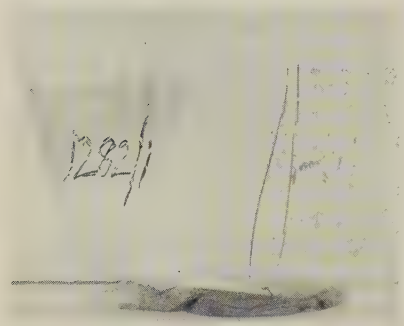

Fig. 6. Synthetic quartz crystal (no. 1282) immersed in benzene, showing freedom from flaws and inclusions. (Dark lines are the wires which suspended the seed plate.)

Under optimum conditions, using single-crystalline seeds, twinning is never found, but when the rate of growth exceeds the critical value Dauphiné twinning may occur. This normally results in the appearance of a major rhombohedral face where the minor rhombohedral face should occur. No examples of Brazilian twinning have been observed. Growth on a twinned seed (whether Brazilian or Dauphiné) results in a similarly twinned growth, the twin boundary being propagated parallel to the optic axis.

Morphology.

The morphology of synthetic quartz grown on to Z-cut seeds follows closely that of natural quartz in most respects. The forms which commonly occur on natural quartz are: $m\{10\bar{1}0\}$, $R\{10\bar{1}1\}$, $r\{01\bar{1}1\}$, $s\{11\bar{2}1\}$, $x\{51\bar{6}1\}$. Trapezohedra other than x are recorded, e.g. $\{41\bar{5}1\}$ and $\{31\bar{4}1\}$, but forms other than m, R, r, s, x are very rarely observed. The R face is often bright and smooth and larger than the complimentary r face which is frequently dull or even matt. The m faces are usually striated in a direction perpendicular to the optic axis.

The forms which occur on synthetic quartz depend on the orientation and shape of the seed plate and on the amount of quartz which has been deposited on it. When growing on a square seed plate cut parallel to (0001) having sides parallel to $(1\bar{1}00)$ and $(11\bar{2}0)$ the following association of forms develops: $m\{10\bar{1}0\}$, $R\{10\bar{1}1\}$, $r\{01\bar{1}1\}$, $a\{11\bar{2}0\}$, $o\{11\bar{2}2\}$, and the trapezohedron of indices $\{h1\bar{h}\overline{+1}1\}$ where h is not greater than 8.

The stereographic projections of right-handed natural and synthetic quartz crystals are shown in fig. 7. Due to the square shape of the seed plate on which the quartz has been deposited, it will be seen that a new zone of faces has appeared on the synthetic crystal. The zone axis for these faces is $[1\bar{1}0]$ and it contains the forms $a\{11\bar{2}0\}$ and $o\{11\bar{2}2\}$. Not

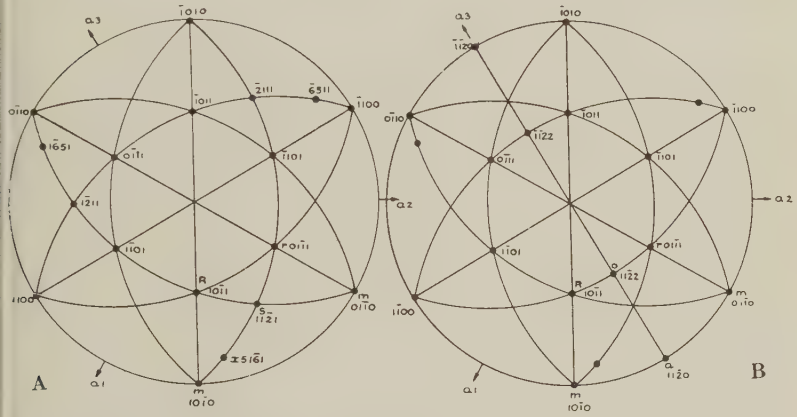

FIG. 7. Stereographic projections of right-handed quartz crystals: A, natural; B, synthetic.

all the faces corresponding to the forms a and o appear but only those which are parallel to one of the edges of the original plate, i.e.

a $(11\bar{2}0)$, $(\bar{1}\bar{1}20)$,
o $(11\bar{2}2)$, $(11\bar{2}\bar{2})$, $(\bar{1}\bar{1}2\bar{2})$, $(\bar{1}\bar{1}22)$.

These forms show an interesting difference at the two ends of the diad axis, a_3. Quartz is more rapidly deposited at the end of the diad axis at which the trapezohedral faces do not develop and hence the $(\bar{1}\bar{1}20)$ face is smaller than the $(11\bar{2}0)$ face at the opposite end of the axis. The trigonal pyramids o are considerably more developed at the fast-growing end of the diad axis and in many cases the faces $(11\bar{2}2)$ and $(11\bar{2}\bar{2})$ are completely absent. The forms o and a are only intermediate forms in the development of the crystal and tend to disappear as the crystal grows. This is shown by the drawing of a typical fully-grown crystal in fig. 8. It may be noticed that the s form $\{11\bar{2}1\}$ which frequently occurs on natural crystals and which is in the same zone as o and a has not been observed on synthetic quartz.

The trapezohedral form which occurs on a right-handed synthetic quartz crystal is prominent only at the negative end of the diad axis

which is parallel to an edge of the seed plate. It is often rounded or striated, but where goniometric measurements have been possible it has been found that it has indices varying between $\{51\bar{6}1\}$ and $\{81\bar{9}1\}$.

The face (0001) is never found, but the growing surface of the crystal remains approximately perpendicular to the optic axis. It develops a characteristic cobbled appearance as shown in fig. 9. The bounding edges often project above the mean (0001) plane which passes through the centre of the growing face.

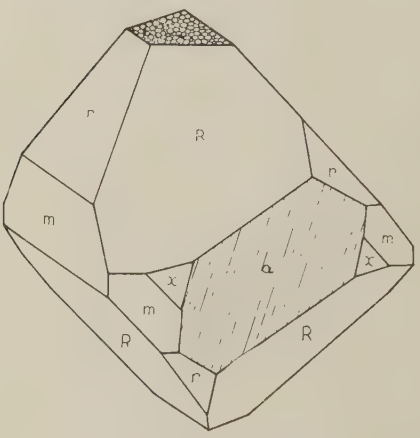

Fig. 8. Habit of a typical synthetic crystal.

The surfaces of the rhombohedral faces on natural quartz show many varied growth features, but those shown on synthetic crystals are, on the whole, of a very simple nature. The partial development of vicinal faces gives rise to conical hills; a particularly clear example found on a *R* face is shown in fig. 10. On the other hand, the prism faces of synthetic crystals are rarely found to be striated.

Where optical measurements could be made without serious disturbance due to vicinal faces, the interfacial angles have been found to correspond with those of natural quartz within the usual accuracy of measurement.

Physical Properties.

To assist in the appraisal of the synthetic quartz which has been grown by the temperature-gradient method a number of the physical properties have been measured and compared with the best-grade natural quartz from Brazil.

Optical properties.—Measurement of the refractive indices on an Abbe refractometer employing a total-reflection method has shown no differences in the indices of natural and synthetic quartz to within the experimental error of $\pm 0{\cdot}0002$. A prism has been cut from a crystal so that when used on a spectrometer part of the light from the collimator passes through synthetic quartz and the remainder through natural quartz. In this way it has been found that the chromatic dispersion is the same for the two materials.

Measurement of the absorption curves in the ultra-violet and infra-red regions has shown some very interesting results. Ultra-violet measurements have been made in the Schumann region from 220 mμ using a vacuum grating spectrograph. In the infra-red, measurements have been made from 1·5 μ using both a Perkin-Elmer spectrometer and a Grubb-Parsons automatic recording spectrometer.

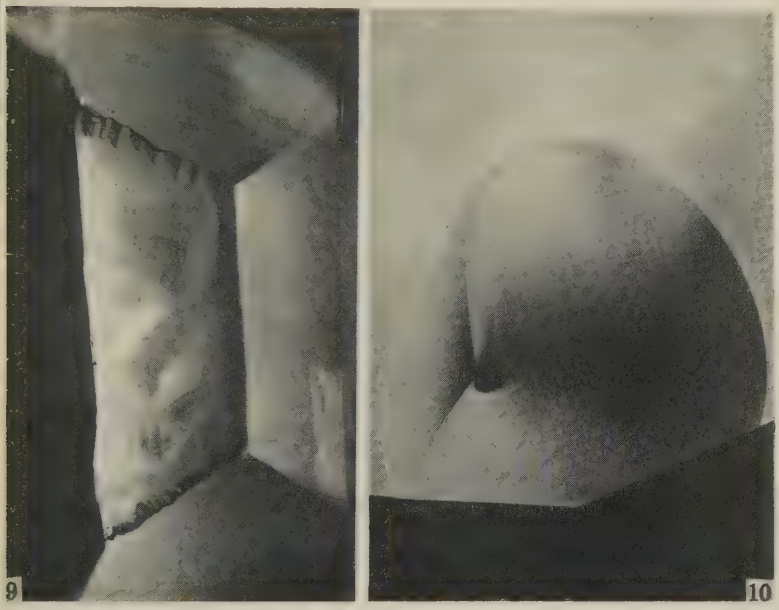

Fig. 9. Cobbled surface approximating to (0001) with adjacent rhombohedral faces. ×5.

Fig. 10. Growth feature on a major rhombohedral face R $(10\bar{1}1)$. ×6·3.

Three synthetic crystals have been examined and compared with a specimen of high-quality natural quartz. Specimen 1 was a crystal showing no sign of Tyndall scattering in a high-intensity light beam, specimen 2 showed scattering of medium intensity, and specimen 3 showed strong scattering. The results for the infra-red region are shown by the curves for percentage transmission against wave-length given in fig. 11. Specimen 1 has a curve similar to that of the natural quartz crystal including the characteristic absorption band at 2·95 μ. Specimens 2 and 3 show a broad absorption band centred about 3·2 μ, this band being more intense in specimen 3. This absorption band and the

associated Tyndall scattering could be explained by the presence of sub-microscopic liquid inclusions. For example, if the resultant absorption of these inclusions was equivalent to a thin film of water, say 0·01 mm. thick, this would give rise to an absorption band extending from about 2·75 μ to 3·5 μ.

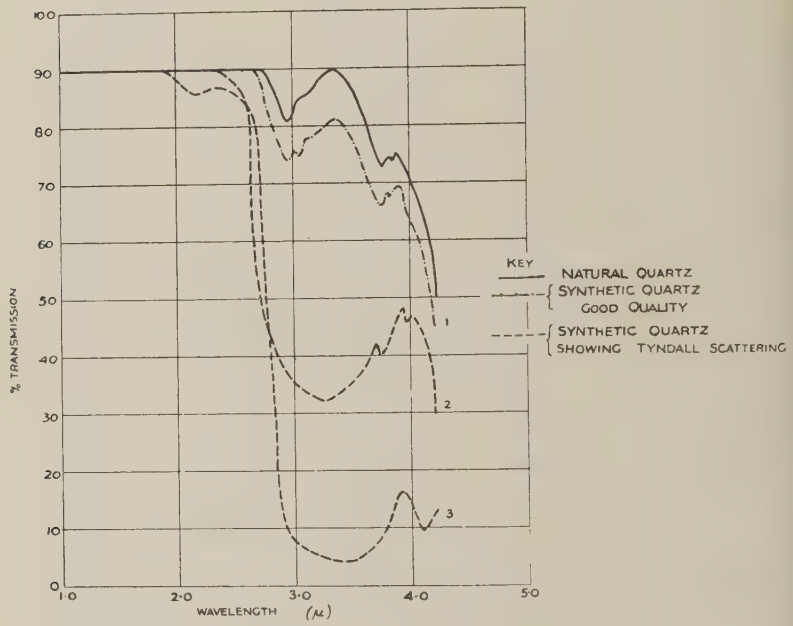

Fig. 11. Infra-red transmission curves through 1 mm. of natural and synthetic quartz.

A somewhat similar trend in the behaviour of the three specimens is shown by the measurements in the ultra-violet region, the cut-off extends farther into the ultra-violet as the degree of scattering lessens. Table I shows approximate wave-lengths for 50 % transmission through 1 mm. of quartz.

Table I. Ultra-violet transmission through 1 mm. of quartz.

Specimens.	Wave-length for 50 % transmission.
High quality natural Brazilian quartz	150 mμ
Synthetic specimen 1	165 mμ
„ „ 2	180 mμ
„ „ 3	193 mμ

Remembering the variations that occur in natural quartzes, synthetic

quartz free from Tyndall scattering would appear to be broadly similar to natural quartz in regard to its spectral transmission.

Using a half-shadow polarimeter, it has been shown that the rotary polarization of natural and synthetic quartz is the same to 0·01°/mm. for the sodium D lines.

Electrical properties.—The performance of piezoelectric oscillator plates cut from the synthetic crystals is not only of practical importance, but it is perhaps the best guide to the overall quality of the material.

Early measurements were carried out on small low-frequency bars which were the only type that could be fabricated from the crystals available at the time. These were found to compare favourably with similar natural quartz bars. A thorough comparison has been carried out more recently using very thin high-frequency plates which provide the most stringent test. The latest of these synthetic oscillator plates are as good as natural quartz, but earlier plates cut from crystals showing Tyndall scattering were considerably poorer than their natural counterparts.

Although a complete study has not yet been carried out to determine the elastic constants, the above work has shown that the frequencies of synthetic and natural quartz oscillators of identical size are the same to within one part in a thousand.

Direct static measurements of the piezoelectric constant d_{11} has shown that the values for natural and synthetic quartz are the same to within 1%.

Other properties.—A comparison of the densities of specimens of natural and synthetic quartz has been carried out using a very sensitive suspension method capable of detecting a difference of two parts in a hundred thousand between two specimens (Douglas and Jones, 1948). Measurements to date on a number of specimens do not indicate any significant difference between the mean densities of natural and synthetic quartz, or in the spread of values about the mean figure.

Comparative hardness figures were obtained using a Vickers microhardness tester using a load of 20 grams. It is difficult to obtain accurate hardness measurements on a crystalline material like quartz. Large loads (about 1 kg.) cause brittle fracture to occur, whereas with small loads such as were used in these measurements elastic recovery may occur giving results which are too high. The results obtained agree to 5%, which is within the experimental error for this type of measurement.

Preliminary measurements have been carried out on the inversion temperature between α- and β-quartz for natural and synthetic powders.

Samples of crushed natural quartz and of a mixture of natural and synthetic quartz were heated simultaneously in a twin calorimeter of a differential thermal analysis apparatus. No difference in the inversion points has been detected to within $\pm 1^\circ$ C.

In addition to the observation of Tyndall scattering, the perfection of the synthetic quartz has been studied using the X-ray topograph technique (Wooster and Wooster, 1945). No difference has been observed in the quality of the best natural and synthetic quartz. At the same time comparison of the lattice spacings has shown no difference to within one part in six thousand.

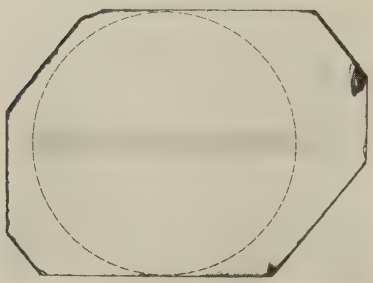

FIG. 12. Section through a synthetic quartz crystal after X-ray irradiation over the area bounded by the broken circle. The darkened region corresponds to the natural quartz seed.

Synthetic quartz grown by the standard temperature-gradient process does not darken when exposed to X-rays even when quite long exposures are used. This result is illustrated by fig. 12, which shows a section of a synthetic crystal grown on a seed plate of natural quartz. Only the central part of the section, corresponding to the natural seed, shows any darkening (Brown and Thomas, 1952).

Work on the removal of Dauphiné twinning from quartz had previously shown that the degree of darkening of natural quartz when exposed to X-ray irradiation was dependent on its perfection and the deeper the darkening the more difficult the crystal was to untwin (Wooster, Wooster, Rycroft, and Thomas, 1947). Synthetic quartz grown under conditions which do not produce the highest quality crystals does darken when exposed to X-rays, but the type of darkening may be different to that found in natural quartz. For instance, quartz grown by the isothermal method darkens to a purple colour similar to that of amethyst. Quartz into which impurities such as copper and arsenic have been introduced is found to darken in a non-uniform manner which is presumably related to the distribution of impurities in the crystal.

CONCLUSIONS.

The work reported here has led to the development of a process capable of producing synthetic quartz crystals which are, in every way,

as good as the best Brazilian quartz crystals. Crystals, weighing up to 150 grams and with growths of up to 16 mm. in the direction of the optic axis on each side of a seed crystal cut parallel to the basal plane, have been grown in about four weeks. The quality of these crystals is dependent on the rate of growth, and below a certain critical value the crystals are completely free from all flaws and twinning.

The physical properties of synthetic quartz have been compared with high-quality natural quartz and it has been found that, except for the behaviour under X-ray irradiation, the properties of the two materials are very similar. The non-susceptibility of synthetic quartz under X-ray irradiation is the only known means of distinguishing the two materials and may be evidence for the supposition that the best synthetic material is more perfect than most natural quartzes.

The present work may throw some light on the rate of growth of large natural quartz crystals. The conditions for the production of flawless synthetic quartz crystals are critical, and it would therefore appear that the best natural crystals must have grown under conditions which did not vary over a wide range.

To estimate the time taken for natural quartz crystals to grow would require a knowledge of the supersaturation and temperature of growth, both of which are very difficult to estimate. It can, however, be concluded from this work that in nature quartz may have grown relatively rapidly; a large natural crystal may have taken only a few years to grow. These conclusions, of course, apply only to natural crystals which have grown under hydrothermal conditions and not to crystals which have been grown from the melt or from vapour.

The authors are indebted to Mr. W. R. S. Garton of Imperial College of Science and Technology, London, Dr. A. E. Martin of Sir Howard Grubb, Parsons & Co., and Mr. W. J. R. Merren of Messrs. Pilkington Bros. for their kindness in carrying out spectral transmission measurements. They also wish to acknowledge the help provided by the British Non-Ferrous Metals Research Association in measuring the hardness of certain synthetic quartz specimens. It is a pleasure to record the valuable advice and encouragement given to the authors by Mr. J. W. Ryde, F.R.S., throughout the course of this investigation.

References.

Brown (C. S.), Kell (R. C.), Thomas (L. A.), Wooster (Nora), and Wooster (W. A.), 1951. Nature, vol. 167, p. 940. [M.A. **11**–367.]

Brown (C. S.) and Thomas (L. A.), 1952. Nature, vol. 169, p. 35. [M.A. **11**–488.]

Bruhns (W.), 1889. Neues Jahrb. Min., vol. ii, p. 63.

Chroustschoff (K. von.), 1887. Bull. Soc. Franç. Min., vol. 10, p. 31; Compt. Rend. Acad. Sci. Paris, vol. 104, p. 602.
Daubrée (A.), 1857. Ann. d. Mines, vol. 12, p. 287; Études et expériences synthétiques sur le métamorphisme. Paris, 1860.
Day (A. L.) and Shepherd (E. S.), 1906. Amer. Journ. Sci., ser. 4, vol. 22, p. 297.
Douglas (R. W.) and Jones (G. A.), 1948. Trans. Soc. Glass Tech., vol. 32, p. 309.
Fenner (C. N.), 1912. Journ. Washington Acad. Sci., vol. 2, p. 471.
—— 1914. Zeits. Anorg. Chem., vol. 85, p. 133.
Hale (D. R.), 1948. Science, vol. 107, p. 393.
—— 1949. Faraday Soc. Discuss., no. 5, p. 189 and p. 363.
Nacken (R.), 1945. F.I.A.T. Final report, no. 641, p. 11. [M.A. **11**–86.]
Schafhäutl (C. E.), 1845. Gelehrte Anzeigen, Akad. Wiss. München, vol. 20, p. 578.
Sénarmont (H. de), 1849. Ann. Chim. Phys., vol. 28, p. 693.
—— 1851. Ann. Chim. Phys., vol. 32, p. 129; Compt. Rend. Acad. Sci. Paris, vol. 32, p. 409.
Spezia (G.), 1900. Atti Accad. Sci. Torino, vol. 34, p. 631.
—— 1905. Ibid., vol. 40, p. 534.
—— 1906. Ibid., vol. 41, p. 158.
—— 1909. Ibid., vol. 44, p. 1.
Thomas (L. A.), Wooster (Nora), and Wooster (W. A.), 1949. Faraday Soc. Discuss., no. 5, p. 341.
Walker (A. C.) and Beuhler (E.), 1950. Indust. Eng. Chem., vol. 42, p. 1369. [M.A. **11**–268.]
Wooster (Nora) and Wooster (W. A.), 1945. Nature, vol. 155, p. 786.
—— —— 1946. Nature, vol. 157, p. 297. [M.A. **10**–104.]
—— —— Rycroft (J. L.), and Thomas (L. A.), 1947. Journ. Inst. Elect. Eng. vol. 94, p. 927.

X-ray investigation of bredigite.

By Audrey M. B. Douglas[1], M.A., Ph.D., A.Inst.P.

Department of Mineralogy and Petrology, University of Cambridge.

[Read November 1, 1951.]

Introduction.

THE X-ray work described below has been done on crystals of bredigite obtained from two different sources, the natural mineral from Scawt Hill, County Antrim, and the synthetic mineral from spiegeleisen slags. Both types of material have been fully described by Tilley and Vincent (1948). Their analysis shows that the slag mineral is a calcium orthosilicate in which Ca is partly replaced by Mg, Mn, and Ba, the extent of the replacement being represented by the formula $(Ca_{1\cdot59}Ba_{0\cdot08}Mg_{0\cdot31}Mn_{0\cdot09})SiO_4$. Tilley and Vincent conclude that this orthorhombic (pseudo-hexagonal) phase is identical with the high-temperature form α' of pure Ca_2SiO_4, the existence of which was suggested by Bredig (1943a), and confirmed by Trömel (1949) using a high-temperature powder camera. Bredig (1943a) also suggests, on the basis of a comparison of X-ray powder patterns, that the crystal structure of α'-Ca_2SiO_4 is similar to that of β-K_2SO_4. The present single-crystal work was originally undertaken in order to investigate the structure of α'-Ca_2SiO_4 more fully.

Unit-cell determination, and relationship between bredigite and pure α'-Ca_2SiO_4.

The orthorhombic (pseudo-hexagonal) symmetry of bredigite was confirmed, and the cell dimensions found for the natural and the synthetic minerals were the same within the limits of experimental error.[2] These are quoted in table I, together with the cell dimensions given by Bredig (1950) for pure α'-Ca_2SiO_4 at 700° C., and also the cell dimensions of β-K_2SO_4. It will be seen that, allowing for the larger ionic radius of K^+ compared with Ca^{2+}, the cell dimensions of β-K_2SO_4 correspond with those reported by Bredig for α'-Ca_2SiO_4, but that the

[1] Hertha Ayrton Research Fellow of Girton College, Cambridge.

[2] The crystals obtained from rock sections were too imperfect for anything but an approximate determination of cell dimensions, and all further work was done on the slag mineral.

a and b dimensions found for bredigite are approximately twice those reported by Bredig for pure α'-Ca_2SiO_4.

Table I. Orthorhombic unit-cell dimensions.

Phase.	Cell dimensions in Å. a.	b.	c.	b/a.	Content of unit cell.
Bredigite (Scawt Hill) ...	10·93±0·05	18·41±0·07	6·75±0·02	1·69	16
Bredigite (slag)	10·91±0·03	18·41±0·05	6·76±0·02	1·69	
α'-Ca_2SiO_4 at 700° C. (Bredig, 1950) ...	5·30	9·55	6·78	1·80	—
β-K_2SO_4	5·73	10·01	7·42	1·75	4
α'-Ca_2SiO_4 at 750° C. ...	11·08±0·05	18·55±0·07	6·76±0·02	1·68	—

The latter discrepancy may arise, not from any real difference between bredigite and α'-Ca_2SiO_4, but because the dimensions for bredigite were obtained from single-crystal photographs, while those for α'-Ca_2SiO_4 were obtained from powder photographs taken by Trömel. The single-crystal photographs show that the intensities of reflections with h and/or k odd (for the large unit cell) are in general weaker than those with h and k even, and thus powder lines corresponding to the former reflections might not have been detected. In an attempt to resolve this point, high-temperature photographs of pure α'-Ca_2SiO_4, taken by Trömel and kindly loaned to the author, were examined, and it was not found possible to assign indices to all the observed lines on the basis of the cell dimensions given by Bredig. A fairly satisfactory interpretation was obtained using the cell dimensions given in the last line of table I, in which it will be seen that the a and b dimensions are approximately, but not exactly, twice those given by Bredig. At least six weak lines cannot be indexed at all if these a and b dimensions are halved.

This observation, however, does *not* establish the identity of bredigite and α'-Ca_2SiO_4, since visual comparison of the two powder photographs shows some marked differences in the two patterns. It seems unlikely that this is due purely to differential thermal expansion, since Trömel's photographs show that little change takes place in the pattern of α'-Ca_2SiO_4 between 750° C. and 1000° C. It is more probable that there is a real, though probably a small, structural difference between bredigite and the α'-Ca_2SiO_4 prepared by Trömel. This structural difference, if it exists, is probably not due to the presence of metallic elements other than Ca in bredigite, since powder photographs of synthetic Ca_2SiO_4 prepared and quenched from 1790° C. by Rait and Goldschmidt (1945) are practically identical with the bredigite pattern. It is there-

ore concluded that the exact relationship between bredigite and the phases occurring in the pure Ca_2SiO_4 system is not yet definitely established, and that this point requires further investigation, which the author hopes to be able to undertake.

Number of atoms per unit cell. The observed density of the slag mineral is 3·40 ± 0·02 gm./c.c. (Tilley and Vincent, 1948), and the number of formula units per unit cell is 16. This result is in agreement with the predicted relationship to the β-K_2SO_4 structure for which the number of formula units is 4 (see table I).

Space-group.—Systematic absences among the X-ray reflections show that the lattice is primitive, and that there is a diagonal glide-plane perpendicular to the z-axis. The first crystal to be examined, extracted from the vugs of the slag, appeared to have a pseudo-diagonal glide-plane perpendicular to the y-axis, that is, there were only a few $h0l$ reflections for which $(h+l)$ was odd, the strongest being 401. Later, evidence was found that these reflections were due, at least in part, to the presence of an extra phase in these bredigite crystals. Crystals afterwards obtained from sections appeared to be free from this extra phase, and a Weissenberg photograph showed that $(h+l)$ was even for all observed $h0l$ reflections except for 401 which was extremely weak. The appearance of this reflection may be due to the presence of a trace of the extra phase, or it may be a real effect, for which an explanation must be sought when the structure analysis has been carried farther.

For the purposes of the structure determination it will be assumed for the present that the glide-plane perpendicular to the y-axis is real, and that the space-group is therefore either $Pmnn$ or $P2nn$. If the space-group is $Pmnn$ all zones of reflections will be centric, whereas if the space-group is $P2nn$ the $h0l$ and $hk0$ zones of reflections will be acentric. Application of the distribution method (Howells, Phillips, and Rogers, 1950) to the observed $hk0$ reflections indicates that this zone is centric (see fig. 1), and thus there is a strong probability that the space-group is $Pmnn$. As the structure analysis proceeds this question will be examined more fully.

The space-group for β-K_2SO_4 is $Pmcn$. Taken in conjunction with the doubling of the a and b dimensions, the difference between the space-groups for bredigite and β-K_2SO_4 indicates a difference between the structures which must involve more than slight displacements of corresponding atoms.

Preliminary work on the structure of bredigite.—An ($hk0$) Patterson projection has confirmed the similarity of the array of Ca and Si atoms

in bredigite and the K, Na, and S atoms in glaserite. It also indicates two possible arrangements of the oxygen atoms, one of which resembles the arrangement in glaserite. Further work to determine the exact nature of the structure is now proceeding.

Orientation of the Indicatrix.—Tilley and Vincent (1948) suggested an arbitrary definition of the optic axial plane as (100) and the prismatic cleavages as (110), thus making $b \simeq \sqrt{3}a$, which is in accordance with the

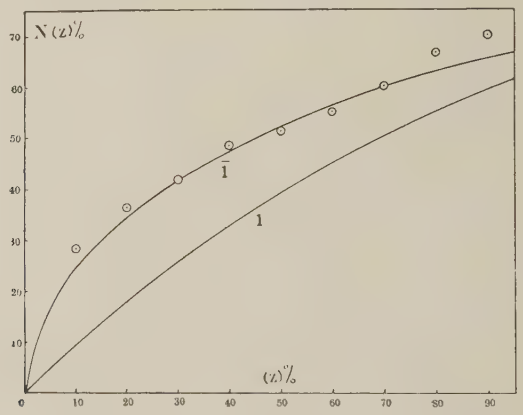

Fig. 1. Intensity distribution curve for the $hk0$ reflections from bredigite. (z) = intensity of a reflection expressed as a percentage of the average intensity, $N(z)$ = percentage of reflections having intensities $\leqslant (z)$. Curve marked $\bar{1}$ is the calculated distribution for a centric zone, and that marked 1 is the calculated distribution for an acentric zone. ⊙ experimental points.

unit cell of table I. However, direct comparison of the optical and X-ray results from several crystals (both single and twinned) showed that the optic axial plane is in fact (010) (acute bisectrix parallel to z). The cleavage plane thus becomes (130), and the common form of twinning is on (110) not on (130). The latter is also in accordance with X-ray observations, since, of the four twinned crystals examined, all were twinned on (110).

The extra phase present in crystals of the slag mineral.

Several bredigite crystals were extracted from vugs in the slag. A number of these proved to be single crystals of the orthorhombic phase, but X-ray photographs, particularly Weissenberg photographs, showed the presence of a few extra reflections, fainter and broader than those

of the main pattern, and always in the same position with respect to the latter.

It was not possible to interpret these extra reflections in terms of either of the twin laws observed by Tilley and Vincent (1948). To confirm this, two twinned crystals were extracted from slag sections, and both gave X-ray patterns which could be interpreted on the basis of twinning on (110). Comparison of (*hk*0) Weissenberg photographs of these and the crystals from the vugs showed that while the pattern from the major component of the twinned crystal matched exactly the main pattern from the 'single' crystal, the reflections from the minor component of the twinned crystal did not coincide with the broad extra reflections. Although no crystals showing twinning on (130) were obtained, so that a similar direct test was impossible, calculation showed that the extra reflections were not due to twinning on this plane.

The possibility that the extra reflections were due to the presence of one of the other phases found in the slag, monticellite (orthorhombic), melilite (tetragonal), and calcium sulphide (cubic), was also considered, but in no case did the positions of the reflections accord with the published X-ray data.

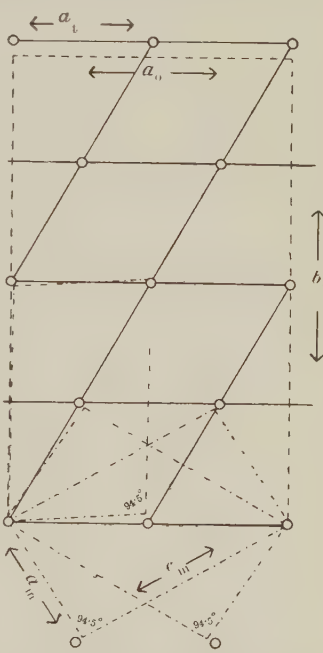

Fig. 2. Relative orientations of the trigonal, orthorhombic, and monoclinic lattices.
—— Trigonal lattice ⊥ *c*-axis,
– – – Orthorhombic lattice ⊥ *c*-axis,
–·–·– Monoclinic lattice ⊥ *b*-axis,
○ Pairs of cations which overlap in this projection in all three structures.

The only satisfactory interpretation of the extra reflections which could be found was that they were due to a small amount of a trigonal phase in fixed orientation relative to the main orthorhombic crystal. The cell dimensions of this phase compared with those of bredigite are $c_t \doteq c_o = 6{\cdot}76$ Å., $a_t = a_o/2 = 5{\cdot}46$ Å., and $\sqrt{3}\, a_t = 9{\cdot}46$ Å., where $b_o = 9{\cdot}21$ Å., the subscripts *t* and *o* denoting the trigonal and orthorhombic phases respectively. The relative orientations of the two lattices are such that $a_t \parallel a_o$ and $c_t \parallel c_o$ (see fig. 2). Examination of the *hk*0, *hk*1, *hk*2,

and $hk3$ Weissenberg photographs suggests that the Laue symmetry of the extra phase is $\bar{3}m$, and the association of the extra reflections with the strongest of the $hk0$ reflections from bredigite indicates that there is probably a strong resemblance between the two structures when projected along the z-axis (this is not surprising considering the strongly pseudo-hexagonal nature of the z-axis of bredigite). These observations suggest that the extra phase is in fact the α-form of Ca_2SiO_4. High-temperature powder investigations by Trömel (1949) and Van Valkenburg and McMurdie (1947) have shown that this phase has a trigonal unit cell, and according to Bredig (1941, 1942) it has a trigonal structure identical with that of glaserite, $K_3Na(SO_4)_2$. The Laue symmetry of glaserite is $\bar{3}m$, and the projections along z of structures of this mineral and of bredigite have been shown to be probably very similar (see below).

The trigonal phase was not observed optically by Tilley and Vincent either in the original investigation (1948) or in a re-examination of crystals which had been used in this X-ray work. However, detection of this phase would be difficult owing to the close similarity of the optical properties of the trigonal and orthorhombic phases (see table III), and the uniaxial character of the trigonal phase may be masked by stresses present in the bredigite crystal. In addition, the relative intensities of the X-ray reflections show that only a small amount of the trigonal phase is present. What little there is may be in the form of particles which, though in parallel orientations, are very small and are distributed throughout the specimen. This assumption of small particle size (or of inhomogeneous strain, see above) is supported by the observed broadening of the X-ray reflections.

No trigonal phase was detected in five crystals extracted from sections of the slag, whereas no crystal extracted from a vug failed to show the extra X-ray reflections characteristic of the trigonal phase. Some suggestions may be made to account for the apparent difference in trigonal phase content in the vugs and in the main body of the slag. It may be due to differences in composition which could influence the phases stable at room-temperature in two ways, first by affecting the nature of the phase in equilibrium at a constant high temperature, and second by altering the rate of inversion on cooling (cf. Bredig, 1950). It could also be due to different rates of cooling in the two parts of the slag, or to a combination of the two effects.

The cell dimensions of the trigonal phase associated with bredigite are compared in table II with those reported by other workers for the α-Ca_2SiO_4 phase either at high temperature or stabilized by the addition

of various oxides. It will be seen that the a dimension agrees reasonably well with the other reported values, but c and hence c/a differ from the rest by about 5%.

This difference is of the same order as reported by Bredig (1943b) for the discontinuous change in the c/a ratio on heating trigonal $KNaSO_4$. Bredig attributes this increase in c/a for $KNaSO_4$ (and also the thermal effects observed by other workers) to the onset of rotation of the SO_4 group. For this compound there is no change in crystal system when the axial ratio changes, but Bredig suggests that for several other compounds, including Ca_2SiO_4, rotation of the anion group starts simultaneously with the transition from the orthorhombic to the trigonal form. He further remarks that no obvious explanation can be given for the observation that c/a is the same for pure α-Ca_2SiO_4 at 1500° C. (in which the anions are presumed to rotate) and for the stabilized α-phase at room-temperature (in which the anions would not be expected to rotate). It follows that the most direct interpretation of the differences in c and c/a, which are seen in table II, is that in the trigonal phase

Table II. Trigonal unit-cell dimensions.

Phase.	Cell dimensions in Å.			Reference.
	a.	c.	c/a.	
α-Ca_2SiO_4 at 1500° C.	5·45	7·18	1·32	Bredig, 1950
α-Ca_2SiO_4 at 1500° C.	5·47**	7·19**	1·31	Van Valkenburg & McMurdie, 1947
Ca_2SiO_4 containing Al_2O_3 and Na_2O	5·45*	7·03*	1·29	Greene, 1944
Ca_2SiO_4 containing Fe_2O_3 and Na_2O	5·41*	7·01*	1·30	Greene, 1944
$7CaO.P_2O_5.2SiO_2$	5·39*	7·11*	1·32	Bredig, 1943a
Phase associated with bredigite	5·46±0·02	6·76±0·02	1·24	—

* Calculated on the assumption that the original figures are given in kX.
** Recalculated from Van Valkenburg and McMurdie's data.

associated with bredigite crystals the anions are not rotating, but have taken up positions in accordance with the space-group symmetry. By contrast, it would appear that in the other stabilized α-Ca_2SiO_4 structures at room-temperature the anions, though not actually rotating, occupy statistically the positions corresponding to rotation, and so the c/a ratio does not change from its value at high temperatures. All these suggestions must, however, remain very tentative until accurate X-ray intensity data are available, from which definite conclusions can be drawn about the positions of the atoms.

The relationship between the α, α', and β structures.

Detailed information is available for only one of the structures of Ca_2SiO_4, that of the β-form, larnite, which has been solved by Mrs. Midgley (1952). O'Daniel and Tscheischwili (1942) have shown that the γ-form has an olivine-type structure, while Bredig has predicted structural similarity between α-Ca_2SiO_4 and $K_3Na(SO_4)$, and between α'-Ca_2SiO_4 and β-K_2SO_4. The preliminary structure work described in this paper is in agreement with these predictions. On the basis of the knowledge so far available, it thus seems very probable that the structures of the trigonal (α), orthorhombic (α'), and monoclinic (β) forms of Ca_2SiO_4 are very similar to one another, while the transition to the γ-form involves a considerable rearrangement of the atoms. Optical data and measurements of cell dimensions support this view (see table III).

Table III. Physical characters of the modifications of calcium orthosilicate.

	α-Ca_2SiO_4.	α'-Ca_2SiO_4.	β-Ca_2SiO_4.	γ-Ca_2SiO_4.
Mineral name... ...	—	Bredigite	Larnite	Calcio-olivine
Crystal system ...	Trigonal	Orthorhombic	Monoclinic	Orthorhombic
Refractive indices α ...	1·724 [1]	1·713 [2]	1·707 [3]	1·642 [4]
β ...	1·724 [1]	1·717 [2]	1·715 [3]	1·645 [4]
γ ...	1·738 [1]	1·732 [2]	1·730 [3]	1·654 [4]
Optic axial angle 2V...	0 [1]	~ 30° [2]	~ 74° [3]	60° [4]
Cell dimensions in Å. a	5·46 [1]	10·91 [2]	5·48 [3]	5·06 [6]
b	— [1]	18·41 [2]	6·76 [3]	11·28 [6]
c	6·76 [1]	6·76 [2]	9·28 [3]	6·78 [6]
β	—	—	94·5° [3]	—
Volume in Å.^{3} ...	½(346)	4(339)	344	387
Contents of unit cell...	Ca_2SiO_4	$16Ca_2SiO_4$	$4Ca_2SiO_4$	$4Ca_2SiO_4$

[1] Beliankin and Lapin, 1946. Data obtained from $(Ca_{1\cdot58}Mg_{0\cdot32}Fe_{0\cdot10})SiO_4$.
[2] Tilley and Vincent, 1948. Data obtained from $(Ca_{1\cdot59}Ba_{0\cdot08}Mg_{0\cdot31}Mn_{0\cdot09})SiO_4$.
[3] Tilley, 1929. Data obtained from Ca_2SiO_4 containing only a trace of Al_2O_3, FeO, and MgO.
[4] Quoted by Tilley, 1929. Data obtained from synthetic Ca_2SiO_4.
[5] Midgley, 1952.
[6] O'Daniel and Tscheischwili, 1942.

Mrs. Midgley (1952) has described the relatively small atomic movements involved in transitions from one to another of these three similar structures. This proposed mechanism of phase change would lead one to expect certain relative orientations between any two phases where they exist in conjunction.

The relative orientation of the trigonal and orthorhombic lattices, determined directly from X-ray photographs as described above, agrees with that predicted from the structures (see fig. 2). The relative orienta-

tion of the monoclinic and orthorhombic lattices could not be found directly, since no single crystal was available in which the monoclinic phase was present in conjunction with another phase. Instead, the relative orientation was found indirectly in the following manner. First the optic axial plane of larnite was found, by X-ray and optical observation of the same crystal, to be near (100), according to Midgley's (1952) choice of axes, and γ is parallel to the y-axis. The prominent twin lamellae were shown to be parallel to (100). These results are in agreement with those reported by Tilley (1929). Tilley and Vincent (1948) find several examples of larnite associated with bredigite in the Scawt Hill mineral, and give drawings showing the relative orientation of the twin lamellae of larnite and the optic axial plane of bredigite. In one case twin lamellae are at $\pm 30°$ to the optic axial planes of the two portions of a twinned bredigite crystal, and in another case the twin lamellae are at 90° and $\pm 30°$ to the bredigite optic axial plane. In all cases the acute bisectrices for larnite and bredigite were parallel, that is the y-axis of larnite is parallel to the z-axis of bredigite. In a plane at right angles to this direction the above data indicate that there are three possible orientations of the monoclinic relative to the orthorhombic lattice, and these are shown in fig. 2. They are in accordance with the postulated mechanism of phase change. The circles indicate the pairs of cations which overlap or partially overlap in this projection of all three structures. The anions and other cations are omitted in order not to confuse the diagram.

The fact that bredigite has been found in conjunction with larnite, and also apparently with the trigonal phase, is in agreement with Trömel's findings that for pure Ca_2SiO_4 and for Ca_2SiO_4 containing 10% ($Na_2O+Al_2O_3+CaO$) the trigonal phase is stable at high temperatures, the orthorhombic phase stable at intermediate temperatures, and the monoclinic phase metastable at low temperatures (Trömel and Möller, 1950). However, it is perhaps surprising to find three orientations of the monoclinic phase if this has, in fact, been formed from the orthorhombic phase, since two of these orientations are equivalent, but the third requires slightly different atomic shifts. The three orientations are, however, exactly equivalent if the monoclinic phase forms directly from the trigonal phase (cf. Tilley and Vincent, 1948, p. 262). On the evidence presented in this paper it is unfortunately impossible to decide whether the trigonal α-phase has formed from the orthorhombic α'-phase on cooling, or vice versa.

It would therefore appear (see also Greene, 1944, and Bredig, 1950)

that the equilibrium and metastable states of Ca_2SiO_4, especially when other cations are present, require a considerable amount of further investigation.

Acknowledgements.—I wish to express my thanks to Professor C. E. Tilley, Dr. S. O. Agrell, and Dr. W. H. Taylor for the interest they have taken in this work. I should also like to thank Dr. G. Trömel and Mrs. C. M. Midgley for their co-operation in loaning X-ray photographs and material. Invaluable assistance has been given by Mr. Kenneth Rickson, who has taken most of the X-ray photographs.

Summary.—Preliminary work has been done on the structure of the mineral bredigite, and it has been shown that while the structure is similar to, it is not identical with, that of β-K_2SO_4. The X-ray investigation has shown the presence in some bredigite crystals of a small quantity of a trigonal phase which could not be detected optically. The optic axial plane, twin planes, and cleavage plane have been determined unambiguously. The relative orientations of the trigonal, orthorhombic, and monoclinic phases are discussed in relation to their structures.

References.

Beliankin (D. S.) and Lapin (V. V.), 1946. Compt. Rend. (Doklady) Acad. Sci. URSS, vol. 51, p. 705. [M.A. **10**–106.]

Bredig (M. A.), 1941. Journ. Amer. Chem. Soc., vol. 63, p. 2533.

—— 1942. Journ. Phys. Chem., vol. 46, p. 747.

—— 1943a. Amer. Min., vol. 28, p. 594. [M.A. **9**–92.]

—— 1943b. Journ. Phys. Chem., vol. 47, p. 587.

—— 1950. Journ. Amer. Ceram. Soc., vol. 33, p. 188.

Greene (K. T.), 1944. Journ. Research Nat. Bur. Standards, U.S.A., vol. 32, p. 1.

Howells (E. R.), Phillips (D. C.), and Rogers (D.), 1950. Acta Cryst., vol. 3, p. 210.

Midgley (C. M.), 1952. Acta Cryst. (in press).[1]

O'Daniel (H.) and Tscheischwili (L.), 1942. Zeits. Krist., vol. 104, p. 124. [M.A. **8**–290.]

Rait (J. R.) and Goldschmidt (H. J.), 1945. Journ. Iron & Steel Inst., vol. 151, p. 391.

Tilley (C. E.), 1929. Min. Mag., vol. 22, p. 77.

—— and Vincent (H. C. G.), 1948. Min. Mag., vol. 28, p. 255.

Trömel (G.), 1949. Naturwiss., vol. 36, p. 88.

—— and Möller (H.), 1950. Forts. Min., vol. 28 (for 1949), p. 80. [M.A. **11**–470.]

Van Valkenburg (A. *Jr.*) and McMurdie (H. F.), 1947. Journ. Research Nat. Bur. Standards U.S.A., vol. 38, p. 415.

[1] I am indebted to Mrs. Midgley for allowing me to see her paper prior to publication.

Changes in habit during the growth of baryte crystals from the north of England.

By A. F. Seager, B.Sc., A.K.C., F.G.S.
Department of Geology, Birkbeck College, University of London,
and W. F. Davidson, F.G.S.

[Read November 2, 1950.]

SOME specimens of baryte, recently obtained from Westmorland, show up to six changes of habit during growth. This was elucidated with the aid of the colour-zoning and fluorescent zones. A change of habit is also recorded in one specimen from County Durham.

Occurrence.

Silverband mine, near Knock, Westmorland.—The coloured crystals, which show numerous habit-changes, were found in a small unnamed vein running obliquely between the Dunfell and Henrake veins, two of the chief veins in the mine. The deposit occupies a considerable replacement area at the base of the Great Limestone. Bands of limonite and psilomelane occur in the vein, the former being abundant. The lower bands of limonite have druses containing clear, colourless, tabular crystals of baryte. Coloured baryte crystals are found in the higher oxide bands, but are mainly confined to the uppermost band, while occasionally they are found for a distance of a few feet in the limestone above. The doubly-terminated crystals are found mainly on the roofs of the druses, while those which are singly-terminated occur on the floors and the lower parts of the sides. Druses containing small, clear fluorite crystals are found. Galena is also present.

Cowgreen mine, Harwood-in-Teesdale, County Durham.—A number of specimens from this mine show groups of thin rectangular crystals, with no visible change of habit; they are tabular on *c*, and bounded mainly by *d*, *o*, *a*, *b*, and *m*, the last three forms being subordinate in size. Elongation is in the direction [100]. The crystals, although colourless and transparent, possess a finely 'frosted' appearance, due to etching.

A single specimen, discovered recently, has a yellow overgrowth on *o*, and presumably on *b*, tending to complete the prism laterally, as in stage 3 of the baryte from Silverband mine. The yellow overgrowth is

not fluorescent. This specimen was found at the 106-feet level in the Greenhush vein in the Melmerby Scar Limestone. This east–west baryte vein carries some ankerite and calcite, as well as small quantities of chalcopyrite, galena, and blende.

Crystallography of baryte from Silverband mine.

Stage 1.—The forms are represented by the conventional letters: *a*{100}, *b*{010}, *c*{001}, *m*{110}, *d*{102}, and *o*{011}. The earlier-formed

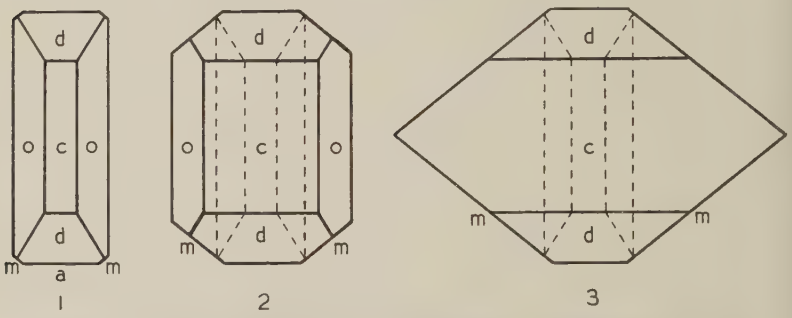

Figs. 1–3. Baryte crystals from Silverband mine, Westmorland, showing successive stages of growth.

crystals, which compose the cores of those showing changes of habit, are of the type usually found at this mine, and shown as stage 1 (fig. 1). The habit is not absolutely constant and the degree of elongation in the direction [100] is somewhat variable. The form *a* is fairly common, while *b* is less so, and {*hkl*} forms are rare. Sometimes the crystals show morphological hemimorphism. One exceptional crystal is elongated in the direction [110]. Such variations are not common and the normal habit is well represented by stage 1. The constancy of the habit during growth in this stage is attested by the presence of a fine, grey, powdery deposit on *d* in some crystals, giving closely-spaced ghost-zoning. Apart from inclusions the crystals are colourless, with a high degree of transparency. Liquid inclusions are not evident. A very minor habit-change sometimes occurs, whereby *a* is partly and *b* completely eliminated by a semi-opaque white overgrowth.

In this stage the most rapid growth takes place on *m* and *d*, as shown by the direction of elongation. Most of the colourless ghost crystals are between 2 and 8 cm. in length.

Stage 2.—At this stage the first major habit-change occurs. Growth stops on *m*, *d*, and *c*, but proceeds on *o*. This initial overgrowth is

ellowish-brown, sometimes with a tinge of green. When viewed through parallel to *o* the overgrowth is seen to consist of closely-spaced yellowsh-brown and colourless zones. An occasional very thin blue zone ccounts for the greenish tinge. When viewed normal to *c* the colour of he crystal appears homogeneous. If *a* was originally present it is liminated at this stage.

Stage 3.—The further growth on *o* is pale blue in colour, and again hows zoning. This is continued until *o* finally disappears. Since stage 1

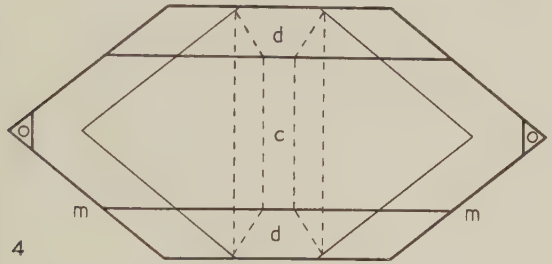

4

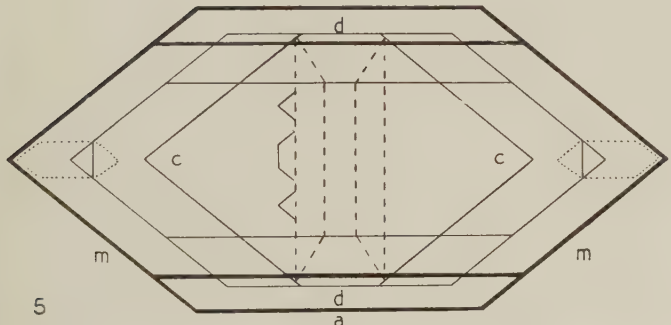

5

a

FIGS. 4 and 5. Baryte crystals from Silverband mine, Westmorland, showing later and final stages of growth.

here has been a considerable extension of *c*, *d*, and *m* at the expense of , but no growth, or virtually none, has taken place on the first three of hese forms. The cessation of growth on *c*, *d*, and *m* can be seen from the istribution of the coloured overgrowth, and is indicated with even reater clarity for the latter form by the transitional ghosts outlined ithin the crystal by fine particles of an impurity. In one such series of hosts a bipyramid can be seen.

There are occasional exceptions to the uniform blue overgrowth on *o*.

In some cases it is so pale that the colour is barely perceptible, in others reversion to a yellowish-brown colour marks the final growth on *o*, while one specimen shows a clear green succeeding blue in the closing phase of stage 3.

Most of the crystals are singly-terminated, the width of the crystal, as measured from the centre of the colourless ghost to the tip of the blue zone, ranging from about 1·5 to 6 cm., depending on the length of the ghost crystal.

Stage 4.—After the cessation of growth on *o*, following its elimination, deposition starts on *m*. This takes place in such a way that *o* reappears. The overgrowth on *m* is very closely zoned, showing a succession of thin layers with differences of colour, hue, or transparency. The earliest zones, which are very pale blue, are followed by an alternating series of yellow and colourless zones, yellow predominating in the later zones. Minute solid inclusions also form a number of ghost zones in this stage. The thickness of the very pale blue zone is about 4 mm. and that of the yellow and colourless zones together is about 5 mm.

Stage 5.—This is the final stage in the growth of the baryte crystals from Silverband mine. Growth continues on *m* and *o*, but as *o* is now growing fast relative to *m* (the converse of stage 4) this results in the second and ultimate disappearance of *o*. Growth now starts on *d*, leading to the reappearance of *a*. For the majority of crystals this is the first time that growth has taken place on *d* since stage 1, although a few crystals show a thin yellowish-brown layer which was deposited at the beginning of stage 2. The whole of this new growth is white and semi-opaque, but the last millimetre of it is least translucent of all, and forms a white layer on the surface of *m*, *d*, and *a*. Variations in the degree of translucency give rise to banding parallel to *m*. The semi-opaque white overgrowth on *m* and *d* is about 7 mm. thick. The total width of a doubly-terminated crystal at the end of stage 5 varies from about 8 to 20 cm. No new growth has taken place on *c*.

Stoppage of growth.

A few crystals have passed successively through all the stages from 1 to 5, some only reached stage 4, others only stage 3, while the rest did not grow beyond stages 1 or 2. Apart from two exceptions, to be described below, no specimens show the omission of one or more stages during growth from stage 1 to stage *n*, although *n* may have any value up to 5 for different specimens. Thus, while some specimens were passing

through the whole series of changes from stages 1 to 5, others had their growth terminated at earlier points in the series.

It is interesting to consider what may have caused the cessation of growth at different times. It is known from the experiments of Bunn[1] and Humphreys-Owen[2] that crystal faces may stop growing while in contact with a solution of sufficient supersaturation to cause growth. In such cases the stoppage depends on some property of the face, and not of its environment. After an interval of time the faces may be observed to start growing again. That this is not the explanation in the case of the baryte crystals here described seems clear from the fact that the pauses in growth observed by Bunn and Humphreys-Owen (loc. cit.) were of relatively short duration, and therefore would not explain the long periods involved here. It appears that crystals in different places were cut off from contact with the solution at different times, so that the habits of stages 1 to 4 represent final habits for some crystals, but only transitional habits for others, while stage 5, the end of the series, is only reached by a few crystals.

In the course of this work over thirty specimens have been examined, and only two of them show the omission of a stage or stages during growth. One shows the habit of stage 2, the other of stage 3. Both have a fluorescent overgrowth which is thickest on *o*, thinner on *d*, and a mere film on *m*. It is completely absent from *c*. This distribution of the fluorescent overgrowth, and particularly its appearance on *d*, strongly suggests that it was formed during stage 5. Thus, although all the crystals were probably cut off from the solution at different times, it appears that in a few cases contact was re-established at a later period.

Inclusions in stages 2 to 5.

All stages of the overgrowths show long, cloudy, linear inclusions. Microscopic examination shows them to be trains of liquid inclusions. In stages 2 and 3 the inclusions seem to be parallel to (100), but, as they can only be seen through *c*, it is difficult to be certain whether they are parallel to the *b*-axis or normal to *o*. They do not appear to be sufficiently inclined to be normal to *o*. Microscopic observation, using the calibrated fine adjustment, does not solve the problem, as the trains of

[1] C. W. Bunn, Discussions of the Faraday Society, 1949, no. 5, p. 136 et seq. [M.A. 11–337.]

[2] S. P. F. Humphreys-Owen, Discussions of the Faraday Society, 1949, no. 5. pp. 145 and 148. [M.A. 11–337.]

inclusions have too great a depth and too ill-defined an outline on the upper and lower surfaces to make measurement possible.

In stages 4 and 5 the inclusions seem to be normal to *m*, that is, they are parallel to the direction of growth. When the colour in stage 3 is faint, such as that at the beginning of stage 4, so that the boundary between the two stages is not definable with certainty, the orientation of the inclusions provides the necessary evidence.

Where a large train of inclusions reaches the surface in stage 3 it can often be seen that a similar train in stage 4 starts from the same point. It is interesting that such a series of inclusions should be continued, although changed in direction by some 51°.

When one of the trains of inclusions in stages 2 and 3 reaches the surface of *c* it tends to form a line of low vicinal pyramids. When etching has been extensive the trains of inclusions also form directions of preferential solution, which lead to the development of channels parallel to the *b*-axis. Etching is much less common, and when present it is less extensive on *c* of the colourless ghost than on the coloured overgrowth, suggesting greater structural perfection in the former.

Vicinal pyramids on *c* are much more numerous on the areas of coloured overgrowth than on the colourless ghost. This provides a sensitive test for the absence of appreciable further growth on *c* of the ghost. The facts just mentioned, together with the inclusions in stages 2 to 5, suggest a much more rapid growth in these stages than in stage 1.

Interesting solution effects are seen in one crystal, representing an early phase of stage 5, in which there is an overgrowth about one millimetre thick on *d* and *c* (the latter being exceptional in these crystals, in which growth usually stops on *c* at the end of stage 1). It shows marked solution-channels internally on *c* of the blue crystal at the earlier part of stage 3, which are made visible by the presence of minute particles of impurity, although the later clear green growth of that stage in this atypic crystal appears unaffected.

The drawing (fig. 5) of the crystal in stage 5 shows a closed area, marked by dotted lines, near the lateral extremities of the crystal. These areas have been likened to a candle flame in shape and are dark yellow in colour. The figure unavoidably gives the impression of a well-defined outline, which is by no means true in white light. The 'flame' was not easy to interpret, as the distribution of its colour seemed to bear no relation to the forms on which the crystal had grown. The solution of this problem, described below, was only found by the use of ultra-violet light, in which certain zones are fluorescent.

Fluorescence and phosphorescence.

The ultra-violet lamp used in these investigations is specified to emit 95% of its total radiation at 3650 A. The fine, yellow zones deposited on *m* towards the end of stage 4 show a strong cream fluorescence. The whole of the overgrowth in stage 5 on *m*, *a*, and *d* fluoresces white, except the outermost 1 mm. layer of least translucent baryte, which appears to be non-fluorescent.

The 'flame' fluoresces strongly with the same cream colour as the yellow zones on *m*. The outline of the 'flame' is now sharply defined, as shown in the drawing of stage 5, and in some specimens can be seen to consist of alternations of strongly and weakly fluorescent zones on *o*. In ordinary light these strongly fluorescent zones are yellow, and it is the overlapping of the yellow zones on *o* and *m*, when the crystal is viewed through *c*, which produces the 'flame', and gives it such an ill-defined outline. The 'flame' is the trace of *o*, and it shows how *o* reappears during stage 4, maintains a constant size for some time and ultimately disappears again immediately before the end of stage 5.

On some crystals, in which development stops early in stage 4, a minute fluorescent spot appears just below *o*-faces, while no fluorescence appears on *m*-faces. This shows that the earliest fluorescent layers are deposited on *o*, just prior to the first fluorescent zones on *m*.

The yellowish-brown zone, sometimes found succeeding the blue zone at the very end of stage 3, is fluorescent. Only a few crystals show the yellowish-brown 'tip'. The simplest explanation of its appearance is that solutions bearing this coloured impurity arrive towards the close of stage 3, in which the crystals are growing only on *o*. This solution causes the same habit, so growth from it only occurs on those crystals in which *o* has not yet vanished. On the other crystals, mainly the smaller ones, no deposition of yellowish-brown baryte takes place at this stage, as *o* is absent.

One specimen has been seen of crystals which are tabular on *c* and elongated in the direction [010], and bounded by *c*, *d*, *m*, and *o*. They are yellowish-white and semi-opaque in the centre and transparent at the ends, except for internal semi-opaque white patches in similar positions to the 'flame' in crystals of stage 5. They show no sign of colourless ghosts or of colour-zoning. The specimen exhibits a cream-coloured fluorescence throughout, except for the semi-opaque patches, which are a brilliant white, representing zoning on *o*. This appears to be a new generation of crystals formed simultaneously with the later part of

stage 4. There growth is restricted to *o* and *m*, which agrees well with the elongation on [010] in the specimen just described.

In all the Silverband baryte those parts of the crystals which are fluorescent are also phosphorescent, with an afterglow of about four seconds for the brighter zones.

A number of specimens of baryte from Felsőbánya, Romania, were examined. Some showed faint colour-zoning, by no means comparable in depth of colour with the present specimens, and none showed fluorescence.

The mechanism of habit-changes.

Evidence has been obtained from the baryte here described of two distinct morphological mechanisms of habit-change.

1. *The mechanism of gradual habit-change.*

This seems to be the mechanism of many changes of habit, and the one operating throughout in stages 1 to 5, apart from one exception to be mentioned below. Some variation in the environment induces a change in the relative growth-velocities of the forms concerned. A face with a high growth-velocity relative to its neighbours, and to which it is not normal, will decrease in size as growth proceeds, and may ultimately disappear, while the neighbouring faces encroach upon it and grow larger at its expense An example is provided by *o* in stages 2 and 3. Because of its relatively rapid growth this form disappears by the end of stage 3, and thereby much increases the size of the neighbouring faces of *c* and *m*.

2. *The mechanism of abrupt habit-change.*

Inside several crystals from Silverband mine fine serrations, like saw-teeth, may be seen on the edge (011) ($01\bar{1}$) of the colourless ghost, as represented by continuous lines on the ghost drawn in stage 5 (fig. 5). Some are pointed and others are elongated. They are bounded, vertically, by *m*. The other surfaces cannot easily be determined. It is not always possible to say whether the 'teeth' are actually growing on (010), or from the common edge between ($0\bar{1}1$) and ($0\bar{1}\bar{1}$), or very near it. If the former is the case, they are probably bounded by *m* and *o*. If they are growing on *o* the bounding surfaces are probably vicinal {*hhl*} forms.

The morphological result of this type of growth is the very rapid elimination of a particular form, which was presumably unstable under

the new conditions prevailing in the solution at that time. By further growth, and coalescence of the 'teeth', a normal crystal would develop, without re-entrant angles, but of a new habit.

In the Cowgreen mine specimen the apparent basal pinakoid of the yellow overgrowth consists of a number of steep intergrown vicinal forms of the type {*hhl*}, which produce shallow serrations on the surface. Similar markings on crystals in stage 5 from Silverband mine suggest that it was through the development of these vicinal forms that *o* was finally eliminated.

Other examples of this phenomenon are not hard to find. One of us (A. F. S.) has noticed a slight roughness on the basal pinakoid of certain wulfenite specimens, consisting of an overgrowth of a large number of minute pyramidal forms. Among the Yugoslavian wulfenite specimens in the Mineral Department of the British Museum (Natural History) were found examples of the expected habit-change. Specimens from Mežica (= Mies) and Črna (= Schwarzenbach) in Slovenia show simple tabular crystals, transitional habits with numerous minute pyramidal projections, and the final form a bipyramid. In one specimen the tabular, transitional, and bipyramidal habits are found together. The bipyramidal crystals disclose their origin by the difference in colour of the dark orange-red tabular crystal and the paler overgrowth.

Zircon also affords good examples. J. A. Butterfield[1] and F. Smithson[2] record overgrowths on detrital zircon which have formed in situ in sedimentary rocks. The original grains, whether nearly euhedral or much rounded, show elongation in the direction [001]. The habit is long or short prismatic with bipyramidal terminations. The overgrowth is almost entirely bipyramidal, forming minute serrations on the original prism. The prism appears to be less stable in the new environment, and is replaced by numerous small elements of the bipyramid.

Calcite seems to be peculiarly susceptible to changes of habit. One of the authors (A. F. S.) has a number of specimens of calcite showing marked changes of habit. Most of them belong to the gradual type of habit-change, but there are three examples of the abrupt type. One shows a scalenohedron completely overgrown by obtuse negative rhombohedra; another consists of a large positive unit rhombohedron covered by numerous crystals of nailhead habit. The last specimen, from Bleiberg, Carinthia, began as a positive unit rhombohedron of which the lateral edges were bevelled by a scalenohedron, and was later over-

[1] J. A. Butterfield, Geol. Mag., 1936, vol. 73, p. 511. [M.A. 6–432.]
[2] F. Smithson, 1937. Geol. Mag., vol. 74, p. 281.

grown by crystals bounded mainly by the same scalenohedron and an acute negative rhombohedron.

Grateful acknowledgement is made for the facilities granted at the Mineral Department of the British Museum (Natural History) for the examination of baryte from Felsőbánya and wulfenite from Yugoslavia.

The chemistry and mineralogy of the Kinkell tholeiite, Stirlingshire.

By F. Walker, M.A., D.Sc., and H. C. G. Vincent, M.A.
Geology Department, University of Cape Town
and R. L. Mitchell, Ph.D.
Macaulay Institute for Soil Research, Aberdeen.

[Taken as read March 27, 1952.]

Introduction.

THE tholeiite of Kinkell (11 km. north of Glasgow G.P.O.) was described by the first author (Walker, 1930) and an analysis of its residual glass was given in a later publication (Walker, 1935). Since unaltered and separable residual glasses of basaltic rocks are rare, the Kinkell example has been referred to frequently in petrological literature. E. A. Vincent (1950) has made a detailed comparison between the Kinkell glass and a similar one from a tholeiite from Kap Daussy, east Greenland. In view of this and of the important part played by such glasses in discussions on basaltic differentiation, all the major constituents of the Kinkell rock have been isolated and analysed chemically and spectrographically. They are described below together with a fuller account of the field relations of the rock and some comments upon the significance of the new data.

The field work was carried out by the first author (Walker). He is also responsible for writing the article and for the views set forth in it. The separation of the constituent minerals, the determination of their optical properties, and the new chemical analyses are the work of the second author (Vincent), while the third author (Mitchell) estimated the trace elements spectrographically, using the cathode-layer-arc technique (Mitchell, 1940).

Field characters.

The Kinkell tholeiite is exposed in an abandoned quarry lying 400 m. WNW. of the eighth milestone from Glasgow on the Glasgow-Lennoxtown road. This quarry is situated on the southerly curving end of a typical E.-W. dike about 20 m. wide. The dike may be traced eastwards by sporadic outcrops and by underground workings to the 'Riggin'

where it forms a multiple intrusion 30 m. wide (Crampton, 1911, pp. 120–121). Material was collected from the exposures in the river south of Milton and from an old quarry immediately south of Antermony Loch. In both cases types were found which, though more altered, closely matched the rock from the southern part of the Kinkell quarry both in fabric and mineralogical composition. Furthermore, these types bear a close resemblance to specimens from other E.–W. tholeiite dikes from the Midland Valley, particularly those of Newton Hill type (Walker, 1935, p. 146). The unusually fresh Kinkell rock may therefore be considered beyond any reasonable doubt to belong to the Permo-Carboniferous quartz-dolerite dike suite of central Scotland.

As stated in the 1930 description (Walker, 1930, pp. 371–372) the type from the northern part of Kinkell quarry differs from the analysed rock from the southern part by being more glassy and containing late skeletal ilmenite in place of chlorophaeite. It is possible that we are dealing here with a multiple intrusion, but the exposures are too scanty to show any line of demarcation between the two types. A decomposed rock was found along the extreme south of the quarry working which appears to represent the chilled basaltic margin of the southern type and has some bearing on its crystallization history.

In the following account only the southern type from Kinkell quarry will be considered, since its mineral constituents permit of relatively easy separation. A new analysis of this type has been used in the present investigation. It is quoted together with the previous analyses in table III.

Microscopic characters and chemical analyses.

A large amount of fresh material was collected in 1947 from the southern part of Kinkell quarry and many new slides prepared from it. These show some features not recorded in 1930 (Walker, 1930, pp. 371–372) when the microscopical examination of the rock was carried out under less favourable conditions.

The mode of the rock was redetermined (Walker) using a Dollar recording micrometer over a total traverse length of 300 mm. with the following result:

Mode (% by weight) of tholeiite from southern part of Kinkell quarry.

Pyroxene	27·4	Chlorophaeite	4·9
Alagioclase	26·1	Apatite	2·2
Iron ore	13·0	OPal	0·7
Glass	25·7		

The following is an amplification of the 1930 descriptions of the individual mineral constituents.

Pyroxene.— About 99 % of the pyroxene consists of pale-brown augite. Most of this forms composite groups with idiomorphic external boundaries but rather irregular internal boundaries. Isolated grains are idiomorphic and there are also large numbers of acicular microlites in the glass with irregular terminations. The relationship of the augite towards the plagioclase is variable and neither mineral can be said to be idiomorphic towards the other. Simple and lamellar twinning on (100) are common and there is some colour zoning. The average grain diameter is 0·3 mm.

TABLE I. Chemical analysis of augite from tholeiite, Kinkell quarry, Stirlingshire. New analysis. (Analyst, H. C. G. Vincent.)

	Analysis.	Molecular ratios.	Atomic ratios to 6(O,OH).		
SiO_2 ...	50·92	0·8478	Si ... 1·9010		2·00
			Al ... 0·1276	0·099	
Al_2O_3 ...	2·90	0·0285		0·029	
TiO_2 ...	1·18	0·0148	Ti ... 0.0331		1·00
Fe_2O_3 ...	0·47	0·0029	Fe ... 0·0132		
FeO ...	11·11	0·1546	Fe ... 0·3467		
MnO ...	0·33	0·0046	Mn ... 0·0104		
MgO ...	15·63	0·3882	Mg ... 0·8702	0·565	
				0·305	
CaO	17·28	0·3081	Ca ... 0·6907	0·695	1·00
Na_2O ...	0·12	0·0019	Na ... 0·0042		
K_2O ...	0·12				
H_2O+...	0·07		$Ca_{35·76}Mg_{45·06}Fe_{19·17}$		
H_2O-...	nil		Sp. gr. 20° 3·375–3·391		
	100.13		2V 42–50°, β 1·696–1·700, γ:c 42–44°.		

The optical properties given in 1935 (Walker, 1935, p. 141) were confirmed (α 1·699, β 1·708, γ 1·720, 2V 48°), but are now thought to represent the iron-rich end of the range of composition. γ and α were then determined on cleavage flakes and β calculated. The highest values were taken and these were probably measured on microlites which would have a preferential tendency to lie in the required direction and would represent the last and most iron-rich stages of pyroxene crystallization.

A very careful redetermination of β was made using sodium-light and grains giving centred optic axial interference figures. The range of values obtained was 1·696–1·700, the mean figure being 1·698. The

refractive index of the liquid was checked on a Leitz-Jelley refractometer then calibrated against an Abbe refractometer which had been standardized by its reference plate. 2V and $\gamma:c$ were measured on the universal stage on about forty grains, giving a range of values between 42° and 50° with a mean value of 47° for 2V and of 42–44° for $\gamma:c$ (mean 43°). A determination of γ on cleavage flakes gave a range of 1·710–1·720.

In addition to the augite there is a small amount of pigeonite (2V 0–14°) as grains which are almost indistinguishable from the main pyroxene. Professor H. H. Hess, who very kindly examined our slides and who first detected the mineral, put the proportion at 6 %, basing it on the shortfall of the calcium atom ratio below the anticipated value (35·76 % against 38 %) using his curves (Hess, 1949, plate I). Many more sections and grains have since been examined by the first two authors and they consider that 6 % is an overestimate. Of over 200 suitably orientated grains examined only one showed a value within the pigeonite range. The proportion of pigeonite in the total pyroxene is probably under 1 % and the pyroxene analysis has therefore been given uncorrected. It is impracticable to separate the two pyroxenes mechanically owing to their close optical resemblance and their specific gravity overlap.

The composition of the augite expressed as atomic ratios is $Ca_{36}Mg_{45}Fe_{19}$ according to the chemical analysis. Using the curves of Hess (1949, plate I) and Muir (1951, fig. 4) the atomic ratios are respectively $Ca_{38}Mg_{38}Fe_{24}$ and $Ca_{39}Mg_{37}Fe_{24}$. No explanation has yet been found for these discrepancies.

Plagioclase is the most abundant constituent in the rock by volume, being slightly in excess of both pyroxene and glass. It forms idiomorphic tables with Carlsbad, albite, and occasional pericline twinning. There is no trace of alteration and the crystals show only slight zoning confined to the margins. The bulk of the mineral consists of labradorite An_{50-58} with β 1·560, but the extreme margins are more sodic. All of the mineral has a refractive index well above that of Canada balsam and this also applies to the microlitic outgrowths from the terminations. The range of composition, based on specific gravity measurements, is An_{44-57} and the average composition calculated from the analysis (table II) is $Ab_{41·3}An_{55·7}Or_{2·8}Cn_{0·2}$.

The plagioclase is variable in its relations towards the pyroxene, sometimes penetrating it and sometimes being moulded on it. The iron ore, however, is always idiomorphic towards the felspar and is often completely enclosed by it. The absence of true plagioclase microlites

from the glass is noteworthy, but microlitic outgrowths from the terminations of crystals are fairly common.

TABLE II. Chemical analysis of plagioclase from tholeiite, Kinkell quarry, Stirlingshire. New analysis. (Analyst, H. C. G. Vincent.)

SiO_2 ...	... 54·50	Na_2O ...	... 4·41		
TiO_2 ...	... 0·12	K_2O ...	... 0·47		
Al_2O_3 ...	... 29·77	BaO ...	... 0·07	Sp. gr. at 22° 2·673–2·692.	
Fe_2O_3*	... 0·17	H_2O ...	... nil	*FeO and Fe_2O_3 as Fe_2O_3.	
MgO ...	... 0·08	SrO ...	... n.det.	Composition:	
CaO ...	... 10·72			$Ab_{41\cdot3}An_{55\cdot7}Or_{2\cdot8}Cn_{0\cdot2}$.	
			100·31		

Iron ore is one of the most conspicuous constituents in the rock and has two distinct habits. The first and dominant type is of early crystallization forming discrete grains and groupings both of which show idiomorphic outlines. They penetrate both plagioclase and augite, some of the smaller individuals being completely enclosed. The second habit is microlitic and skeletal, the mineral being confined to the glass. It is rare in the analysed rock, but is conspicuous in specimens from the north side of the quarry.

The ore was separated by Clerici solution, one hundred grams of the crushed rock yielding 11 gm. of ore. This is lower than the modal percentage of ore (13·0), but iron ore is one of the most variable constituents of the tholeiite. The separated ore was divided by a hand magnet into two fractions with the following properties:

	(*a*) Highly magnetic fraction.	(*b*) Weakly magnetic fraction.
Weight ...	... 10·1 gms.	0·9 gm.
Sp. gr. ...	... 4·25	3·56
Ti % ...	... 10·47	25·6

These figures suggest that (*a*) is magnetite with some ilmenite and that (*b*) is ilmenite with some magnetite, the ratio of (*a*) to (*b*) in the rock being approximately 10:1.

Examination of polished sections with vertical illumination confirms the above. Both magnetite and ilmenite are present as separate individuals, the latter in much smaller quantity occurring as rounded grains in the magnetite and also as discrete crystals. Positive identification was given by etch tests: tarnishing and isotropic behaviour for the magnetite; and anisotropism and etch tests for the ilmenite. An X-ray powder photograph of the (*b*) fraction was identical with a control photograph of undoubted ilmenite from California and contaminating magnetite lines were not discernible.

The tholeiite also contains pyrite as minute spherical grains nearly all

in the oxide iron ore from which they cannot be separated by physical means. They form 0·48 % of the rock by volume or 0·83 % by weight, as measured micrometrically on a polished section viewed by reflected light. This proportion corresponds to a sulphur content of 0·44 %, a figure which shows reasonable agreement with the 0·33 % determined chemically.

Glass.—Since the glass in the material collected in 1947 was slightly fresher than that isolated in 1935 another separation was made. The separated material was not, however, reanalysed, although fluorine, boron, and baria were determined and are quoted as additions to the 1935 analyses in table III.

TABLE III. Chemical analyses of tholeiites and their residual glasses.

	1.	2.	3.	4.	5.	A.	B.	6.
SiO_2 ...	48·55	49·10	50·2	66·80	72·4	47·42	63·96	50·4
TiO_2 ...	2·94	4·02	3·0	0·18	0·2	3·98	0·78	3·2
Al_2O_3 ...	14·64	12·13	15·1	12·10	13·1	11·75	11·60	12·8
Fe_2O_3 ...	5·42	4·61	5·6	0·97	1·1	3·39	2·93	4·9
FeO ...	8·28	8·92	8·5	1·50	1·6	12·79	2·76	9·4
MnO ...	0·23	0·15	0·2	n.d.	—	0·10	0·05	0·2
MgO ...	3·92	4·50	4·0	0·50	0·5	5·35	1·16	5·5
CaO ...	8·06	8·20	8·3	2·62	2·8	10·83	5·65	9·5
BaO ...	0·08	—	0·1	0·29	0·3	—	—	—
Na_2O ...	2·07	2·14	2·1	2·40	2·6	2·36	1·91	2·2
K_2O ...	1·51	2·10	1·6	4·20	4·6	0·55	1·55	1·2
H_2O+ ...	2·02	2·50	—	5·75	—	0·95	6·12	—
H_2O- ...	1·52	1·02	—	3·00	—	0·30	0·72	—
S ...	0·33	0·03	0·4	—	0·4	—	—	—
P_2O_5 ...	0·83	0·51	0·9	0·39	0·4	0·54	0·96	0·5
CO_2 ...	trace	—	—	—	—	—	—	—
B_2O_3 ...	nil	—	—	nil	—	—	—	&c.
ZrO_2 ...	nil	—	—	—	—	—	—	&c.
F ...	0·07	—	—	0·01	—	—	—	0·2
	100·47	99·93	100·0	100·71	100·0	100·31	100·15	100·0
	0·03							
	100·44	Sp. gr. ...		2·28–2·31	—	2·99	2·43	—

1. Tholeiite, dike, Kinkell quarry, Stirlingshire. New analysis. Analyst, H. C. G. Vincent.
2. Tholeiite, dike, Kinkell quarry, Stirlingshire. Analyst, J. Jakob (Walker, 1930, p. 372).
3. Analysis 1, calculated water free.
4. Residual glass from tholeiite of analysis 2. Analysts, W. H. Herdsman (Walker, 1935, p. 150) with new additions by H. C. G. Vincent.
5. Analysis 4 calculated water free.

A. Olivine-tholeiite, dike, Kap Daussy, east Greenland. Analyst, E. A. Vincent (1950, p. 56).

B. Residual glass from tholeiite of analysis A. Analyst, E. A. Vincent (1950, p. 56).

6. Average of 7 analysed Permo-Carboniferous tholeiites from central Scotland, calculated water free.

The glass separated from the 1947 material agrees in its optical properties with that separated previously (n 1·495). It is now evident, however, that the mineral previously regarded as chlorophaeite of late separation is in reality a product of devitrification of the glass. All transitions between this green mineral and unaltered glass are to be

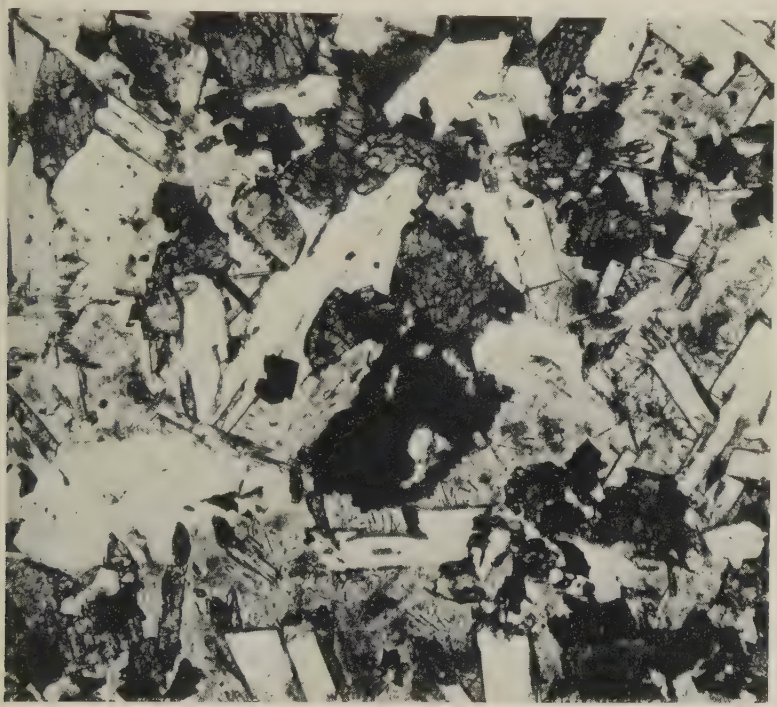

FIG. 1. Photomicrograph of the Kinkell tholeiite, Stirlingshire. A large area of pale glass at the base shows incipient alteration to darker palagonite. Ordinary light × 35.

seen (fig. 1). Except for its isotropic character the green mineral is equivalent to the green chlorite alteration product of the glass from the Kap Daussy tholeiite described by E. A. Vincent (1950, p. 49). It is frequently associated with a little opal.

The glass contains numerous microlites, small idiomorphic prisms of augite, and conspicuous needles of apatite. Inclusions of iron ore and plagioclase are much rarer.

Apatite, as in so many rocks belonging to this suite, is an abundant accessory. The idiomorphic needles are commonest in the glass, but

they frequently penetrate the plagioclase and more rarely the augite. A parallel grouping of needles sometimes occurs and the maximum crystal size recorded was 1·1 by 0·06 mm.

Analyses of Tholeiite.—The new analysis of the Kinkell tholeiite (no. 1, table III) differs from the previous one (no. 2, table III) in its higher alumina and lower titania and potash. Otherwise the analyses show good agreement. Analysis 1 when calculated water free agrees well with that of the average Permo-Carboniferous tholeiite of Scotland apart from the higher alumina of the Kinkell rock.

Trace elements in minerals.

The minor elements in the mineral constituents of the tholeiite are given in table IV in order of ionic radius.

Table IV. Trace elements in tholeiite constituents as parts per million (analyst, R. L. Mitchell) and comparative data.

		Kinkell tholeiite constituents.				Comparisons with Kinkell glass.			
Elements	Ionic radius	Plagioclase	Augite	Iron ore	Glass	Palisades vein (Walker, 1940)	Skaergaard acid (Wager and Mitchell, 1951)	Caledonian acid (Nockolds and Mitchell, 1948)	Average acid (Tröger, 1935)
V^{+4}	0·61 Å.	—	200	1000	5	25	9	80	—
Ga^{+3}	0·62	40	10	20	20	50	33	40	15
Cr^{+3}	0·64	—	—	—	10	14	11	60	3
Mo^{+4}	0·68	—	2	5	2	—	—	—	—
Sn^{+4}	0·74	—	—	—	—	—	—	—	—
Li^{+1}	0·78	2	2	5	1	—	20	20	150
Ni^{+2}	0·78	—	20	30	5	50	9	20	3
Co^{+2}	0·82	—	80	150	—	250	5	15	10
Cu^{+2}	0·83	<10	<10	80	<10	40	200	—	16
Sc^{+3}	0·83	—	30	—	—	1½	10	10	1½
Zr^{+4}	0·87	50	30	—	>1000	—	1200	200	300
Mn^{+2}	0·91	100	2500	5000	150	—	800	350	1000
Yt^{+3}	1·06	—	—	—	30	—	—	—	—
La^{+3}	1·22	—	—	—	30	—	—	—	—
Sr^{+2}	1·27	1200	10	10	2000	50	450	1300	90
Pb^{+2}	1·32	—	—	—	—	12	—	—	—
Ba^{+2}	1·43	300	—	10	3000	30	1100	1300	450
Rb^{+1}	1·49	—	—	—	300	—	—	—	—

Vanadium shows its greatest concentration in the titaniferous iron ore whose V^{+4} (0·61 Å.) is camouflaged by replacing Ti^{+4} (0·64 Å.) in the crystal lattice or is captured in place of Fe^{+3} (0·61). This is in accor-

dance with expectation, for the high proportion of vanadium in titaniferous iron ores has often been recorded. A lesser replacement of the same elements and possibly of Al^{+3} (0·57 Å.) occurs in the pyroxene, but the element is absent from the plagioclase and insignificant in the glass.

Gallium shows no marked concentration in any constituent. The highest proportion is in the plagioclase where Ga^{+3} (0·62 Å.) probably replaces Al^{+3} (0·57 Å.) diadochically. It should be noted, however, that the amount of gallium is somewhat greater than might be expected in a plagioclase of composition An_{56}. Goldschmidt and Peters (1931) record only 3·7 p.p.m. in bytownite, while Nockolds and Mitchell (1948, pp. 547–551) found about 40 p.p.m. of gallium in plagioclases within the andesine range. The amounts in the pyroxene, iron ores, and glass are normal.

The absence of *chromium* in the three minerals and its small proportion in the glass are noteworthy, for the average value for basic rocks is of the order of 300 400 p.p.m. Probably the element entered the early crystallates easily during pre-injection differentiation, took no part in the middle stages of crystallization, and thus showed a minor concentration in the residual liquid as represented by the glass.

Molybdenum occurs in very small proportions showing a concentration in the iron ore. It is possible that it is confined here to the pyrite in view of its marked affinity for sulphur. *Tin* is absent from all constituents.

The proportion of *lithium* is also very small throughout. Its concentration in the iron ore is perhaps due to the presence of magnesium, both elements having the same ionic radius (0·78 Å.).

The distribution of *nickel* and *cobalt* between the mineral constituents is similar. The latter occurs in greater amount, but both show maximum concentration in the iron ore with lesser proportions in the pyroxene. Ni^{+2} (0·78 Å.) probably replaces Mg^{+2} (0·78 Å.) in the pyroxene, but the position of Co^{+2} (0·82 Å.) is doubtful though it possibly substitutes for Fe^{+2} (0·83). It is possible that both nickel and cobalt occur in the pyrite of the rock. The association of cobalt with the pyrite of the Triassic quartz-diabases of Pennsylvania is well marked (A. F. Buddington, personal communication).

The marked concentration of *copper* in the iron ore is again most probably in the pyrite (Wager and Mitchell, 1951, p. 190), the substitution of Cu^{+2} (0·83 Å.) for Fe^{+2} (0·83) in oxides being relatively unimportant. Elsewhere the proportion of copper is insignificant and below the average for that element.

Scandium is confined to the pyroxene where Sc^{+3} (0·83 Å.) occupies the Fe^{+2} (0·83 Å.), Mg^{+2} (0·78 Å.), or Ca^{+2} (1·06 Å.) positions in the structure. The distribution and proportion of the element are normal.

The small amount of *zirconium* in the plagioclase and pyroxene is probably in zircon which, however, was not recorded microscopically. The marked concentration of this element in the silicic residual glass is normal.

The proportion of *manganese* in the rock (0·23 % MnO) is normal and there is a marked concentration of the element in the pyroxene and iron ore where Mn^{+2} (0·91 Å.) replaces Fe^{+2} (0·83 Å.) diadochically. The proportion in the acid residual glass is lower than the average for granites (500 p.p.m.) and the relatively small amount in the plagioclase doubtless represents minute inclusions of inseparable iron ore rather than diadochic replacement of Ca^{+2} (1·06 Å.) in the felspar structure.

Thallium was recorded in both the plagioclase and the glass, but since Clerici solution was used in the separation process, the results are rendered suspect by the possibility of contamination and are therefore omitted.

Yttrium and *lanthanum* are restricted to the residual glass of the tholeiite which is in accordance with expectation. Their relatively large ionic radius (1·05Å. and 1·06 Å.) prevent substitution for ferrous iron and magnesium in the dark minerals. The amount in the glass is normal.

The distribution of *strontium* and *barium* in the tholeiite is similar, both showing moderate concentration in the plagioclase and a greater concentration (particularly in the case of barium) in the residual glass. This distribution is normal though the proportion of both elements in the tholeiite is above the average and the values may be a little too high. Both Ba^{+2} (1·43 Å.) and Sr^{+2} (1·27 Å.) substitute for K^{+1} (1·33 Å.) in the potash-felspar structure most of which is contained potentially in the residual glass. The lower proportion of barium in the plagioclase structure, where Ba^{+2} (1·43 Å.) and Sr^{+2} (1·27 Å.) are camouflaged replacing Ca^{+2} (1·06) diadochically, is due to the high ionic radius of barium. The lower ionic radius of strontium promotes its incorporation. *Lead* is absent from all constituents of the tholeiite.

Rubidium, like barium, is enriched in the residual glass, owing to its high ionic radius (1·49 Å.), and the proportion is normal. It is camouflaged on crystallization in the potash-felspar structure.

General Comments.—The crystalline constituents of the tholeiite

elong to what may be termed the main stage of crystallization. The ccurrence of about 30 % of glass in the rock gives a clear-cut natural reak between the main stage and what potentially would be the later tages. The chemical composition of the pyroxene, as well as the bsence of chromium, indicate that the earliest crystallates do not enter nto the mineral composition of the rock which, as will be shown below, s slightly advanced along the liquid line of descent from saturated basalt nagma. This is also in keeping with the distribution of the minor lements in the rock, there being very few anomalies.

Crystallization history of kinkell tholeiite.

In his illuminating comparative study of the Kap Daussy and Kinkell holeiites E. A. Vincent (1950) has shown clearly the variation of the nain oxides in the chemical analyses and has given a picture of the ifferentiation trend. The additional data, now presented, allow this icture to be modified in certain respects though the broad outline emains unchanged.

It has been shown above that the minor elements of the Kinkell holeiite behave as expected, entering into the crystal structures or eing concentrated in the residual glass according to their ionic radius nd electrostatic charge. The picture is thus filled in in detail.

Turning to the major constituents Vincent (1950, p. 59) has illustrated he crystallization trends of the two tholeiites and of calc-alkali magma n general by means of the triangular diagram originated by Wager and Deer (1939) with FeO, MgO, and K_2O+Na_2O as co-ordinates. This iagram serves well for intrusions, such as the Skaergaard pluton and he Palisade diabase sill, which are low in Fe_2O_3, but when, as in the Kinkell and Kap Daussy tholeiites, the proportion of ferric oxide is nuch higher the diagram should be modified to include Fe_2O_3 with FeO. This has been done with good effect by Tilley (1950, pp. 52–53) and by H. R. Cornwall (1951, pp. 165–169). The use of molecular proportions Walker 1952) is a further improvement, though it is doubtful whether the additional time involved in calculation is justified in ractice.

The diagram used in fig. 2 has weight percentages of $FeO+Fe_2O_3$, MgO, and Na_2O+K_2O as co-ordinates. It shows all the available uperior analyses of the late Palaeozoic tholeiite province of Scotland nd northern England to which the Kinkell tholeiite belongs. Included mongst these are five new analyses of a differentiated quartz-dolerite ill from Northfield, Stirlingshire (Walker, 1952). Analyses of the

Kap Daussy tholeiite and glass, and of the average rhyolite, dacite, andesite, and basalt of Daly (1933, pp. 9–17) are quoted for comparison, and the new analysis of the Kinkell tholeiite is joined to that of the residual glass by a tie-line.

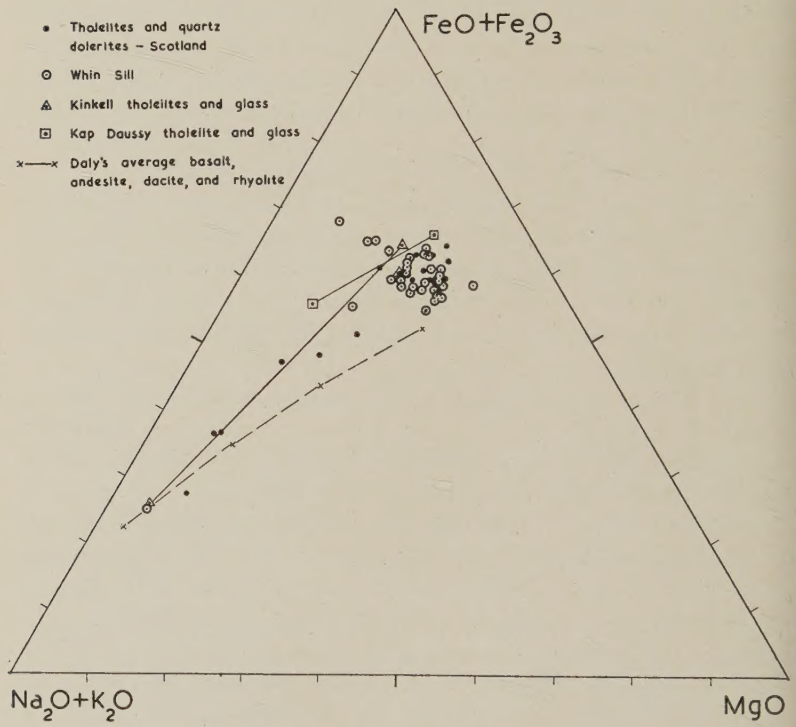

Fig. 2. Crystallization trends of tholeiites.

The two points representing the analyses of the Kinkell tholeiite lie within a closely spaced group of points plotted from analyses of undifferentiated types of the same suite from Scotland and northern England. The chemical composition of the Kinkell tholeiite is thus normal. Furthermore, the tie-lines between either Kinkell tholeiite analyses and that of the residual glass lie just along the line of variation for the suite, proving thereby that the crystallization sequence in the Kinkell rock was again normal.

The corresponding tie-line for the Kap Daussy analyses lies parallel to but slightly above the line of variation for the British suite, as might

e expected in view of the higher degree of fractionation and iron nrichment in the Greenland province.

The variation trend of the British suite lies very close though slightly bove the line joining Daly's averages for rhyolite, dacite, andesite, and asalt (Daly, 1933, pp. 9–17) which represents normal calc-alkali variation. Thus the diagram with total iron as the upper co-ordinate brings ut the normal character of tholeiitic differentiation, whereas, if Fe_2O_3 s omitted for that co-ordinate, the trend-lines in question show considerable separation (Walker and Poldervaart, 1949, p. 659).

The decomposed chill phase of the Kinkell tholeiite shows 8–10 % f phyric plagioclase and augite plainly recognizable by their habit. he two minerals occur in almost equal proportions by volume and it s therefore clear that, when the tholeiite was injected, both constituents ad started to crystallize and formed together under 10 % of solid hase. The normal tholeiite represents a stage where the solid phase ad increased to about 70 % and here too the plagioclase and pyroxene ccur in roughly equal proportions. Evidently the two minerals had he same crystallization range and maintained approximately equal ates of crystallization up to a fairly late stage—a point of some importance. Primary iron ore could not be recognized with any certainty in he decomposed chill phase and thus its crystallization range could not e estimated. It seems, however, to be a fairly early mineral, the rystallization of which tends to build up silica in the residual liquid.

Summary.—The unaltered tholeiite of Kinkell quarry, Stirlingshire, as been reinvestigated and the mineral constituents have been separated and analysed both chemically and spectrographically. No anomalies were found and the distribution of the trace elements in the rock is normal. The two main mineral constituents of the rock—augite and labradorite—had the same crystallization ranges and maintained approximately equal rates of crystallization until the rock was 70 % crystalline.

References.

Cornwall (H. R.), 1951. Differentiation in magmas of the Keeweenawan series. Journ. Geol., vol. 59, pp. 151–172. [M.A. **11**–394.]

Crampton (C. B.), 1911. The geology of the Glasgow district. Mem. Geol. Surv.

Daly (R. A.), 1933. Igneous rocks and the depths of the earth. New York. [M.A. **5**–290.]

Goldschmidt (V. M.) and Peters (C.), 1931. Zur Geochemie des Galliums. Nachr. Gesell. Wiss. Göttingen, Phys. Kl., Fachgruppe IV, no. 11, pp. 165–183, 257–279.

Hess (H. H.), 1949. Chemical composition and optical properties of common clinopyroxenes. Part I. Amer. Min., vol. 34, pp. 621–666. [M.A. **11**–15.]

MITCHELL (R. L.), 1940. The spectrographic determination of trace elements in soils. I.—The cathode layer arc. Journ. Soc. Chem. Industry, vol. 59, pp. 210–213.

MUIR (I. D.), 1951. The clinopyroxenes of the Skaergaard intrusion, eastern Greenland. Min. Mag., vol. 29, pp. 690–714.

NOCKOLDS (S. R.) and MITCHELL (R. L.), 1948. The geochemistry of some Caledonian plutonic rocks . . . and their minerals. Trans. Roy. Soc. Edinburgh, vol. 61, pp. 535–575. [M.A. **10**–424.]

TILLEY (C. E.), 1950. Some aspects of magmatic evolution. Quart. Journ. Geol. Soc. London, vol. 106, pp. 37–61. [M.A. **11**–394.]

TRÖGER (E.), 1935. Der Gehalt an selteneren Elementen bei Eruptivgesteinen. Chemie der Erde, vol. 9, pp. 286–310.

VINCENT (E. A.), 1950. The chemical composition and physical properties of the residual glass of the Kap Daussy tholeiite dike, east Greenland. Min. Mag., vol. 29, pp. 46–62.

WAGER (L. R.) and DEER (W. A.), 1939. Geological investigations in east Greenland, Part III. The petrology of the Skaergaard intrusion, Kangerdlugssuaq, east Greenland. Medd. om Grønland, vol. 105, no. 4, pp. 1–352. [M.A. **8**–27.]

—— and MITCHELL (R. L.), 1951. The distribution of trace elements during strong fractionation of basic magma. Geochim. Cosmochim. Acta, vol. 1, pp. 129–208. [M.A. **11**–495.]

WALKER (F.), 1930. A tholeiitic phase of the quartz-dolerite magma of central Scotland. Min. Mag., vol. 22, pp. 368–376.

—— 1935. The late Palaeozoic quartz-dolerites and tholeiites of Scotland. Min. Mag., vol. 24, pp. 131–159.

—— 1940. Differentiation of the Palisade diabase, New Jersey. Bull. Geol. Soc. Amer., vol. 51, pp. 1059–1105. [M.A. **8**–243.]

—— 1952. Differentiation in a quartz-dolerite sill at Northfield quarry, Stirlingshire. Trans. Geol. Soc. Edinburgh (in press).

—— and POLDERVAART (A.), 1949. Karroo dolerites of the Union of South Africa. Bull. Geol. Soc. Amer., vol. 60, pp. 591–705. [M.A. **11**–32.]